Four-Coordinate, Trigonal Pyramidal Pt(II) and Pd(II) Complexes

Charlene Tsay, Neal P. Mankad, Jonas C. Peters*

Department of Chemistry, Massachusetts Institute of Technology, Cambridge, Massachusetts 02139, and Division of Chemistry and Chemical Engineering, California Institute of Technology, Pasadena, CA 91125

Supporting Information

Experimental Section
Figure S1. Solid-state structures of **1**, **2**, and **3**
Table S1a. Crystal data and structure refinement for **1**
Table S1b. Selected bond lengths and angles for **1**
Figure S2. $^{1}H/^{195}Pt$ 2D HMBC spectrum of **1**
Table S2a. Crystal data and structure refinement for **2**
Table S2b. Selected bond lengths and angles for **2**
Figure S3. $^{1}H/^{195}Pt$ 2D HMBC spectrum of **2**
Table S3a. Crystal data and structure refinement for **3**
Table S3b. Selected bond lengths and angles for **3**
Figure S4. Solid-state structure of **4**
Table S4a. Crystal data and structure refinement for **4**
Table S4b. Selected bond lengths and angles for **4**
Figure S5a. ^{1}H NMR spectrum of **4**
Figure S5b. $^{31}P\{^{1}H\}$ NMR spectrum of **4**
Table S5a. Crystal data and structure refinement for **5**
Table S5b. Selected bond lengths and angles for **5**
Figure S6a. ^{1}H NMR spectrum of **5**
Figure S6b. $^{31}P\{^{1}H\}$ NMR spectrum of **5**
Table S6a. Crystal data and structure refinement for **6**
Table S6b. Selected bond lengths and angles for **6**
Figure S7. $^{1}H/^{195}Pt$ 2D HMBC spectrum of **6**
Figure S8a. ^{1}H NMR spectrum of **7**
Figure S8b. $^{31}P\{^{1}H\}$ NMR spectrum of **7**
Figure S9. $^{1}H/^{195}Pt$ 2D HMBC spectrum of **7**
Figure S10. $^{1}H/^{195}Pt$ 2D HMBC spectrum of **8**
Figure S11. Solid-state structure of **9**
Table S7a. Crystal data and structure refinement for **9**
Table S7b. Selected bond lengths and angles for **9**
Figure S12. $^{1}H/^{195}Pt$ 2D HMBC spectrum of **9**
Table S8a. Crystal data and structure refinement for **10**
Table S8b. Selected bond lengths and angles for **10**
Figure S13. $^{1}H/^{195}Pt$ 2D HMBC spectrum of **10**
Figure S14. UV-visible spectrum of **10**
Figure S15. DFT-calculated frontier molecular orbitals of **10**
Figure S16a. ^{1}H NMR spectrum of **11**
Figure S16b. $^{31}P\{^{1}H\}$ NMR spectrum of **11**
Figure S17. VT ^{1}H NMR spectrum of **11a**
Figure S18. VT ^{1}H NMR spectrum of **11b**
Figure S19. Solid-state structures of **12** and **13**
Table S9a. Crystal data and structure refinement for **12**

Table S9b. Selected bond lengths and angles for **12**
Table S10a. Crystal data and structure refinement for **13**
Table S10b. Selected bond lengths and angles for **13**
Figure S20a. ^{1}H NMR spectrum of **13**
Figure S20b. $^{31}P\{^{1}H\}$ NMR spectrum of **13**
Figure S21. Solid-state structure of **15**
Table S11a. Crystal data and structure refinement for **15**
Table S11b. Selected bond lengths and angles for **15**
Table S12a. Crystal data and structure refinement for **16**
Table S12b. Selected bond lengths and angles for **16**
Figure S22. UV-visible spectrum of **16**
References

Experimental Details.

General Considerations. All manipulations were carried out using standard Schlenk or glovebox techniques under an atmosphere of dinitrogen. Solvents were degassed and dried by sparging with Ar gas and passage through an activated alumina column. Deuterated solvents were purchased from Cambridge Isotopes Laboratories, Inc. and were degassed and stored over activated 3 Å molecular sieves prior to use. Reagents were purchased from commercial vendors and used without further purification unless otherwise noted. $[SiP^{Ph}_3]H$,[1] $[SiP^{iPr}_3]H$,[1] (COD)PdMeCl,[2] and $H(BAr^F_4)\cdot 2Et_2O$[3] were synthesized according to literature procedures. Elemental analyses were performed by either Columbia Analytics (Tucson, AZ) or Midwest Microlab (Indianapolis, IN).

NMR Spectroscopy. ^1H, ^{13}C, ^{19}F, ^{29}Si, and ^{31}P NMR spectra were collected at room temperature, unless otherwise noted, on Varian Mercury 300 MHz, Bruker Avance 400 MHz, and Varian Inova 500 MHz NMR spectrometers. ^{195}Pt resonances were detected indirectly by a $^1H/^{195}Pt$ 2D HMBC experiment at room temperature on a Varian 400 MHz spectrometer with a broadband auto-tune OneProbe. Due to the lower resolution of these 2D spectra, the one-bond Pt-P coupling constants obtained from the corresponding ^{31}P spectra should be considered more accurate. ^1H and ^{13}C spectra were referenced to residual solvent resonances. ^{19}F spectra were referenced to external C_6F_6 (δ = -164.9 ppm). ^{29}Si spectra were referenced to external tetramethylsilane (δ = 0 ppm). ^{31}P spectra were referenced to external 85% phosphoric acid (δ = 0 ppm). ^{195}Pt spectra were referenced by using the "setref" protocol in Varian's VnmrJ software, which derives the chemical shifts from known frequency ratios of the ^{195}Pt standard (1.2M Na_2PtCl_6 in D2O at 0 ppm) to the lock signal of the deuterated solvent.[4, 5]

IR Spectroscopy. IR measurements were obtained from KBr pellets using a Bio-Rad Excalibur FTS 3000 spectrometer with Varian Resolutions Pro software.

X-ray Crystallography. X-ray diffraction studies were carried out at the MIT Department of Chemistry X-ray Diffraction Facility on a Bruker three-circle Platform diffractometer coupled to a Bruker-AXS Smart Apex CCD detector. Data was collected at 100K using Mo Kα radiation (λ = 0.71073 Å). Structures were solved by direct or Patterson methods using SHELXS and refined against F^2 on all data by full-matrix least squares with SHELXL-97.[6] All non-hydrogen atoms were refined anisotropically. All hydrogen atoms were placed at geometrically calculated positions and refined using a riding model, with the exception of the hydrides bound to Pt in **3** and **9** and the para hydrogen of the toluene in **6**. The hydrogen atoms of note in **9** and **6** were located in the difference Fourier synthesis and refined semi-freely, while the hydride in **3** was constrained to a Pt-H distance equivalent to that of **9**. The isotropic displacement parameters of all hydrogen atoms were fixed at 1.2 (1.5 for methyl groups) times the Ueq of the atoms to which they are bonded. All ligand isopropyl hydrogen atoms for **10** could be located in the difference map and were consistent with the calculated position used in the final refinement. All structures contained disorder in either the solvent molecules or the $-CF_3$ groups of the BAr^F_4 anions. All disorders were refined with the help of similarity restraints on equivalent 1-2 and 1-3 distances. Disordered $-CF_3$ groups were modeled as an idealized disorder over two positions rotated 60° from one another, with equivalent fluorine atoms constrained to have equal anisotropic displacement parameters.

DFT Calculations. All DFT calculations were performed while at the Massachusetts Institute of Technology. The single-point and geometry optimization calculations were done with the Gaussian03 suite at the B3LYP level.[7] The LANL2DZ basis set was used for Pt, Si, and P, with diffuse and polarization functions for Si and P. The 6-31G (d,p) basis set was used for C and H. The metal d-orbital parentage assignments of the HOMO and LUMO of **10** were based on the atomic orbital coefficients for respective molecular orbitals. In the case of the HOMO, the coefficients for the d-orbitals of dxy and dx^2-y^2 symmetry were at least an order of magnitude larger than the coefficients for the other d-orbitals. Similarly, for the LUMO, the contribution of the dz^2 atomic orbital is at least an order of magnitude larger than the other d-orbitals. The relative contributions of Pt vs. Si to the HOMO and LUMO were probed by artificially removing/adding an electron from/to the calculated molecular orbitals, without changing any of the orbital coefficients or energies, and determining the distribution of spin density. This method allowed us to roughly conclude that both the HOMO and LUMO are predominantly of Pt character (44% Pt vs. 1% Si and 54% Pt vs. 23% Si, respectively).

Note concerning lack of C,H,N data for the solvent adducts 4, 5, and 13, and the H_2 adduct 11a,b. The cationic solvento adducts **4**, **5**, and **13**, in addition to the H_2 and HD adducts **11a**,**b**, can be generated cleanly and according to NMR spectroscopy by the methods described below, but the fifth ligand is labile under vacuum or slow evaporative drying, and this fact frustrates attempts to obtain reliable C,H,N data. C,H,N data is provided for all other complexes. Crystals selected for X-ray diffraction experiments were representative of the batches of crystals grown for **4**, **5**, and **13**.

Preparation of [SiP$^{Ph}_3$]Pt-CH$_3$ (1). Under a dinitrogen atmosphere, [SiP$^{Ph}_3$]H (0.941 g, 1.16 mmol) and (COD)PtMe$_2$ (0.386 g, 1.16 mmol) were placed in a resealable Schlenk tube with toluene (40 mL). The tube was sealed and heated to 70 °C for 18 h, resulting in a golden yellow solution with some yellow precipitate. The solvent was removed *in vacuo*. To the residues was added diethyl ether (50 mL) under air, and an off-white powder was collected on a frit and washed with additional portions of diethyl ether to yield analytically pure [SiP$^{Ph}_3$]Pt-CH$_3$ (0.997 g, 84%). The complex is stable to air and moisture indefinitely. Crystals suitable for X-ray diffraction were grown by diffusion of petroleum ether vapors into a THF solution. ^{1}H NMR (CD_2Cl_2, δ): 8.51 (d, J = 7.5 Hz, 3H), 7.48 (t, J = 6.8 Hz, 3H), 7.23 (m, 6H), 7.06 (m, 6H), 6.88 (m, 24H), 0.34 (q, $^3J_{P\text{-}H}$ = 6.9 Hz, $^2J_{Pt\text{-}H}$ = 49.6 Hz, 3H, Pt-C*H*$_3$). ^{13}C{^{1}H} NMR (CD_2Cl_2, δ): 153.3 (m) 149.4 (m), 139.1 (m), 133.5 (s, $J_{Pt\text{-}C}$ = 24.6 Hz), 133.2 (m), 132.5 (q, J = 4.5 Hz), 129.9 (s), 128.8 (s), 128.5 (s), 128.1 (m), -35.4 (q, $^2J_{P\text{-}C}$ = 10.1 Hz, $^1J_{Pt\text{-}C}$ = 458 Hz, Pt-*C*H$_3$). ^{31}P{^{1}H} NMR (CD_2Cl_2, δ): 23.2 (s, $^1J_{Pt\text{-}P}$ = 3104 Hz). ^{195}Pt NMR (CD_2Cl_2, δ): -5928 (q, $^1J_{Pt\text{-}P}$ = 3114 Hz). IR (KBr, cm^{-1}): 3051, 2974, 2864, 1580, 1477, 1429, 1304, 1248, 1182, 1126, 1089, 1065, 1027, 907. Anal. Calcd. for $C_{55}H_{45}SiP_3Pt$: C, 64.63; H, 4.44. Found: C, 64.82; H, 5.35.

Preparation of [SiP$^{Ph}_3$]Pt-Cl (2). Under a dinitrogen atmosphere, [SiP$^{Ph}_3$]H (0.631g, 0.776 mmol) and (COD)PtCl$_2$ (0.290 g, 0.775 mmol) were placed in a resealable Schlenk tube with THF (20 mL) and triethylamine (1.5 mL). The tube was sealed and heated to 70 °C for 1.5 h, resulting in a yellow solution with bright yellow precipitate. This mixture was poured under air into a 250 mL separatory funnel with dichloromethane (75 mL). The combined organic fraction was then washed with water (150 mL), sodium bicarbonate (saturated aq. solution, 2 x 150 mL),

and water (150 mL). The cloudy yellow organic fraction was dried over anhydrous magnesium sulfate, filtered through Celite, and evaporated to dryness by rotary evaporation. Diethyl ether (50 mL) was added with stirring, and a bright yellow powder was collected on a sintered glass frit and washed with several portions of diethyl ether to yield spectroscopically pure [SiP^{Ph}_3]Pt-Cl (0.571 g, 71%). Analytically pure material was obtained by recrystallization from dichloromethane/petroleum ether. The complex is stable to air and moisture indefinitely. Crystals suitable for X-ray diffraction were grown by layering a dichloromethane solution with petroleum ether. ^{1}H NMR (CD_2Cl_2, δ): 8.46 (d, J = 7.2 Hz, 3H), 7.56 (t, J = 7.1 Hz, 3H), 7.32 (m, 6H), 7.11 (m, 18H), 6.91 (t, J = 7.7 Hz, 12H). ^{13}C{^{1}H} NMR (CD_2Cl_2, δ): 150.2 (m), 144.1 (m) 137.6 (m), 134.3 (s, J_{Pt-C} = 30.6 Hz), 133.2 (q, J = 8.0 Hz), 132.8 (q, J = 4.2 Hz), 130.8 (s), 129.6 (s), 129.1 (s), 128.2 (q, J = 3.1 Hz). ^{31}P{^{1}H} NMR (CD_2Cl_2, δ): 29.3 (s, $^1J_{Pt-P}$ = 3064 Hz). ^{195}Pt NMR (CD_2Cl_2, δ): -4562 (q, $^1J_{Pt-P}$ = 3057 Hz). IR (KBr, cm^{-1}): 2051, 2874, 2864, 1582, 1479, 1429, 1255, 1186, 1105, 1065, 1028, 999, 910. Anal. Calcd. for $C_{54}H_{42}SiP_3PtCl$: C, 62.22; H, 4.06. Found: C, 62.02; H, 3.88.

Preparation of [SiP^{Ph}_3]Pt-H (3). Under a dinitrogen atmosphere [SiP^{Ph}_3]H (76.7 mg, 94.4 μmol) and Pt(PPh3)4 (117 mg, 94.4 μmol) were dissolved in THF (5 mL) in a resealable Schlenk tube. The tube was sealed and heated to 70 °C for 17 h. Volatiles were removed, and the residues were triturated with diethyl ether (20 mL) under air. An off-white solid was then collected on a sintered glass frit and washed with diethyl ether (2 x 25 mL) to yield analytically pure [SiP^{Ph}_3]Pt-H (54.9 mg, 58%). The complex is stable to air indefinitely. Crystals suitable for X-ray diffraction were grown by diffusion of petroleum ether vapors into a THF solution. ^{1}H NMR (C_6D_6, δ): 8.60(d, J = 7.5 Hz, 3H), 7.41 (d, J = 9.0 Hz, 3H), 7.27 (m, 15H), 6.97 (t, J = 7.6 Hz, 3H), 6.78 (t, J = 7.3 Hz, 6H), 6.63 (t, J = 7.5 Hz, 12H), -6.27 (q, $^2J_{P-H}$ = 19.8 Hz, $^1J_{Pt-H}$ = 782 Hz, 1H, Pt-*H*). ^{13}C{^{1}H} NMR (C_6D_6, δ): 154.3 (dd, J = 19.7 Hz and 37.1 Hz), 150.3 (m), 140.0 (m), 134.7 (s), 133.6 (m), 132.9 (d, J = 4.1 Hz), 130.0 (s). ^{31}P{^{1}H} NMR (C_6D_6, δ): 34.0 (s, $^1J_{Pt-P}$ = 3092 Hz). IR (KBr, cm^{-1}): 3046, 2974, 2858, 1803 (ν_{Pt-H}), 1582, 1479, 1431, 1304, 1248, 1184, 1093, 1065, 1028, 910. Anal. Calcd. for $C_{54}H_{43}SiP_3Pt$: C, 64.34; H, 4.30. Found: C, 64.44; H, 4.21.

Preparation of {[SiP^{Ph}_3]Pt(OEt_2)}{BAr^F_4} (4). Under a dinitrogen atmosphere, [SiP^{Ph}_3]Pt-CH_3 (15 mg, 15 μmol) and $HBAr^F_4$•2Et_2O (15 mg, 15 μmol) were dissolved in Et_2O and stirred for 10 minutes at room temperature, resulting in a red-orange solution. Red-orange crystals suitable for X-ray diffraction were grown by diffusion of pentane vapors into an Et_2O solution. ^{1}H NMR (Et_2O, δ, referenced to Et_2O methyl protons at 1.10): 8.06 (d, J = 6.8 Hz, 3H), 7.73 (s, 8H, *o*-BAr^F_4), 7.48 (s, 4H, *p*-BAr^F_4), 7.36 (m, 3H), 7.27 (m, 9H), 7.14-7.08 (m, 27H). ^{13}C NMR (Et_2O, δ, referenced to Et_2O methyl carbon at 16.0): 163.1 (q, $^1J_{B-C}$ = 50 Hz), 144.9 (m), 143.5 (m), 136.0 (s), 135.8 (m), 134.1 (m), 133.5, (s) 133.4 (s), 132.1 (s), 132.0 (m), 131.7 (s), 130.5 (q, $^2J_{F-C}$ = 32 Hz, -CF_3), 130.0 (m), 125.8 (q, $^1J_{F-C}$ = 272 Hz), 118.4. ^{31}P NMR (Et_2O, δ): 51.8 (s, $^1J_{Pt-P}$ = 3119 Hz). ^{19}F{^{1}H} NMR (Et_2O, δ): -61.4 (s)

Preparation of {[SiP^{Ph}_3]Pt(CH_2Cl_2)}{BAr^F_4} (5). Under a dinitrogen atmosphere, [SiP^{Ph}_3]Pt-CH_3 (15 mg, 15 μmol) and $HBAr^F_4$•2Et_2O (15 mg, 15 μmol) were dissolved in 5 mL CD_2Cl_2 and stirred for 5 minutes at room temperature, resulting in an orange solution. Pentane vapors were diffused into a CH_2Cl_2 solution at -35 °C to afford {[SiP^{Ph}_3]Pt(CH_2Cl_2)}{BAr^F_4} as orange crystals, which were then crushed and briefly dried under vacuum. Orange crystals suitable for

X-ray diffraction were grown by diffusion of petroleum ether vapors into a CH_2Cl_2 solution. ^{1}H NMR (CD_2Cl_2, δ): 8.15 (d, J = 7.2 Hz, 3H), 7.73 (m, 8H, *o*-$BAr^F{}_4$), 7.60 (t, J = 7.5 Hz, 3H), 7.56 (s, 4H, *p*-$BAr^F{}_4$), 7.46 (t, J = 7.5 Hz, 3H), 7.39 (m, 3H), 7.32 (m, 6H), 7.13 (m, 12H) 6.98 (m, 12H). ^{13}C{^{1}H} NMR (CH_2Cl_2, δ): 161.9 (q, $^1J_{B\text{-}C}$ = 50 Hz), 144.3 (m), 141.1 (m), 135.0 (s), 134.4 (m), 132.9 (m), 132.6 (m), 132.4 (s), 131.4 (s), 131.1 (s), 130.7 (s), 129.1 (s), 129.0 (q, $^2J_{F\text{-}C}$ = 31 Hz), 124.7 (q, $^1J_{F\text{-}C}$ = 272 Hz), 117.6 (s). ^{19}F{^{1}H} NMR (CH_2Cl_2, δ): -61.3 (s). ^{31}P{^{1}H} NMR (CD_2Cl_2, δ): 46.6 (s, $^1J_{Pt\text{-}P}$ = 3062 Hz).

Preparation of {[SiP$^{Ph}_3$]Pt(toluene)}{BAr$^F_4$} (6). Under a dinitrogen atmosphere, [SiP$^{Ph}_3$]Pt-CH_3 (25 mg, 25 μmol) was suspended in toluene. $HBAr^F{}_4$•$2Et_2O$ (25 mg, 25 μmol) was added as a solid. The mixture was stirred for 10 minutes at room temperature and resulted in a dark orange-brown solution. Pentane vapors were diffused into a toluene solution to afford {[SiP$^{Ph}_3$]Pt(toluene)}{$BAr^F{}_4$} as orange-brown crystals, which were then dried under vacuum. Orange-brown crystals suitable for X-ray diffraction were grown by slow diffusion of pentane vapors into a toluene solution. ^{1}H NMR (toluene-d_8, δ): 8.37 (s, 8H, *o*-$BAr^F{}_4$), 7.72 (d, J = 6.6 Hz, 3H), 7.64 (s, 4H, *p*-$BAr^F{}_4$), 7.11-6.98 (m, 9H), 6.90 (m, 12H), 6.80 (m, 18H). ^{13}C NMR (toluene, δ): 162.6 (q, $^1J_{B\text{-}C}$ = 50 Hz), 143.1 (m), 141.6 (m), 135.4 (s), 134.7 (m), 132.6 (s), 132.4 (s), 132.1 (m), 131.1 (d, J = 17 Hz), 130.6 (s), 130.2 (s), 129.6 (q, $^2J_{F\text{-}C}$ = 31 Hz), 128.9 (s), 125.1 (q, $^1J_{F\text{-}C}$ = 272 Hz), 117.9 (s). ^{19}F{^{1}H} NMR (toluene, δ): -60.6 (s). ^{31}P NMR (toluene-d_8, δ): 53.3 (s, $^1J_{Pt\text{-}P}$ = 3090 Hz). ^{195}Pt NMR (CD_2Cl_2, δ): -3860 (q, $^1J_{Pt\text{-}P}$ = 3079 Hz). Anal. Calcd. for $C_{93}H_{62}SiP_3PtBF_{24}$: C, 56.92; H, 3.18. Found: C, 56.02; H, 2.94.

Preparation of [SiP$^{i\text{Pr}}_3$]Pt-CH_3 (7). Under a dinitrogen atmosphere, [SiP$^{i\text{Pr}}_3$]H (200 mg, 328 μmol) and (COD)$PtMe_2$ (120 mg, 361 μmol) were dissolved in toluene and added to a resealable Schlenk tube. The tube was sealed and heated to 90 °C for 16 h, resulting in a golden-yellow solution. Volatiles were removed and the residues washed with pentane (4 x 1 mL) to yield spectroscopically and analytically pure [SiP$^{i\text{Pr}}_3$]Pt-CH_3 as a pale yellow powder (213 mg, 79%). ^{1}H NMR (CD_2Cl_2, δ): 8.10 (d, J = 6.6 Hz, 3H), 7.36 (d, J = 7.8 Hz, 3H), 7.27 (t, J = 6.9 Hz, 3H), 7.16 (t, J = 7.2 Hz, 3H), 2.59 (m, 6H), 1.02 (m, 18H), 0.65 (q, $^3J_{P\text{-}H}$ = 7.8 Hz, $^2J_{Pt\text{-}H}$ = 51.9 Hz, 3H, Pt-CH_3), 0.43 (m, 18H). ^{13}C{^{1}H} NMR (CD_2Cl_2, δ): 154.4 (m), 147.8 (m), 133.4 (m), 129.4 (m), 128.7 (s), 127.0 (s), 29.1 (s), 18.6 (s), 18.4 (s), -47.7 (q, $^2J_{P\text{-}C}$ = 10.4 Hz, $^1J_{Pt\text{-}C}$ = 458 Hz, Pt-*C*H_3). ^{31}P{^{1}H} NMR (CD_2Cl_2, δ): 25.6 (s, $^1J_{Pt\text{-}P}$ = 2967 Hz). ^{195}Pt NMR (CD_2Cl_2, δ): -6324 (q, $^1J_{Pt\text{-}P}$ = 2982 Hz). Anal. Calcd. for $C_{37}H_{57}SiP_3Pt$: C, 54.33; H, 7.02. Found: C, 53.06; H, 7.11.

Preparation of [SiP$^{i\text{Pr}}_3$]Pt-Cl (8). Under a dinitrogen atmosphere, [SiP$^{i\text{Pr}}_3$]H (25 mg, 41 μmol) and (COD)$PtCl_2$ (16 mg, 43 μmol) were dissolved in toluene and added to a resealable Schlenk tube. Triethylamine (2 drops) was added and the tube was sealed and heated to 90 °C for 18 h, resulting in a pale yellow solution with white precipitate. The solution was filtered through Celite and volatiles were removed to yield spectroscopically pure [SiP$^{i\text{Pr}}_3$]Pt-Cl as a yellow powder (28 mg, 82%). Analytically pure material was obtained by diffusion of pentane vapors into a benzene solution. ^{1}H NMR (CD_2Cl_2, δ): 7.98 (d, J = 6.3 Hz, 3H), 7.47 (d, J = 6.6 Hz, 3H), 7.33-7.26 (m, 6H), 2.75 (m, 6H), 1.13 (m, 18H), 0.68 (m, 18H). ^{13}C{^{1}H} NMR (CD_2Cl_2, δ): 151.3 (m), 143.4 (m), 133.4 (m), 129.9 (t, J = 14.1 Hz), 129.4 (s), 128.1 (s), 28.6 (q, J = 8.0 Hz), 18.7 (s), 18.5 (s). ^{31}P{^{1}H} NMR (CD_2Cl_2, δ): 40.9 (s, $^1J_{Pt\text{-}P}$ = 2979 Hz). ^{195}Pt NMR (CD_2Cl_2, δ): -4439 (q, $^1J_{Pt\text{-}P}$ = 2902 Hz). Anal. Calcd. for $C_{36}H_{54}SiP_3PtCl$: C, 51.58; H, 6.49. Found: C, 51.38; H, 6.47.

Preparation of [SiP$^{i\mathrm{Pr}}_3$]Pt-H (9). Under a dinitrogen atmosphere, [SiP$^{i\mathrm{Pr}}_3$]H (15 mg, 25 μmol) and $Pt(PPh_3)_4$ (37 mg, 30 μmol) were dissolved in toluene and added to a resealable Schlenk tube. The tube was sealed and heated to 90 °C for 18 h, resulting in a golden yellow solution. Volatiles were removed and the residue was washed with Et_2O and cold MeCN to afford [SiP$^{i\mathrm{Pr}}_3$]Pt-H as a yellow solid (15 mg, 75%). Analytically pure material was obtained by slow evaporation of an Et_2O solution. Crystals suitable for X-ray diffraction were grown by slow evaporation of a toluene/pentane solution. ^{1}H NMR (CD_2Cl_2, δ): 8.15 (d, J = 6.6 Hz, 3H), 7.39 (d, J = 7.5 Hz, 3H), 7.29 (t, J = 6.9 Hz, 3H), 7.16 (t, J = 7.5 Hz, 3H), 2.09 (m, 6H), 0.86 (m, 18H), 0.41 (m, 18H), -9.84 (q, $^2J_{P\text{-}H}$ = 19.8 Hz, $^1J_{Pt\text{-}H}$ = 787 Hz, 1H, Pt-*H*). ^{13}C{^{1}H} NMR (CD_2Cl_2, δ): 154.9 (m), 148.9 (m), 133.4 (m), 129.9 (m), 128.9 (s), 126.9 (s), 27.2 (m), 19.0 (s), 18.6 (s). ^{31}P{^{1}H} NMR (CD_2Cl_2, δ): 46.2 (s, $^1J_{Pt\text{-}P}$ = 2914 Hz). ^{195}Pt NMR (CD_2Cl_2, δ): -6039 (q, $^1J_{Pt\text{-}P}$ = 2896 Hz). IR (KBr, cm^{-1}): 3103, 3044, 2975, 2954, 2905, 2866, 1821 ($\nu_{Pt\text{-}H)}$, 1471, 1457, 1426, 1301, 1259, 1235, 1159, 1100, 1030, 1019, 960, 933, 922, 878. Anal. Calcd. for $C_{36}H_{55}SiP_3Pt$: C, 53.79; H, 6.90. Found: C, 53.43; H, 6.88.

Preparation of {[SiP$^{i\mathrm{Pr}}_3$]Pt}{BAr$^F_4$} (10). Under a dinitrogen atmosphere, [SiP$^{i\mathrm{Pr}}_3$]Pt-CH_3 (48 mg, 59 μmol) and HBAr$^F_4$•2Et_2O (60 mg, 59 μmol) were dissolved in CH_2Cl_2 resulting in an immediate color change to a dark purple solution with concomitant effervescence. The solution was stirred for 5 minutes at room temperature. Spectroscopically and analytically pure material and crystals suitable for X-ray diffraction were obtained by slow diffusion of pentane vapors in a CH_2Cl_2 solution, which afforded dark purple crystals of {[SiP$^{i\mathrm{Pr}}_3$]Pt}{BAr$^F_4$} (87 mg, 89%). ^{1}H NMR (CD_2Cl_2, δ): 7.80 (d, J = 7.2 Hz, 3H), 7.72 (m, 8H, *o*-BAr$^F_4$), 7.68 (m, 3H), 7.56 (m, 4H, *p*-BAr$^F_4$), 7.52 (d, J = 7.5 Hz, 3H), 7.44 (t, J = 7.2 Hz, 3H), 3.22 (m, 6H), 1.08 (m, 18H), 0.97 (m, 18H). ^{13}C{^{1}H} NMR (CH_2Cl_2, δ): 161.9 (q, $^1J_{B\text{-}C}$ = 50 Hz), 144.0 (m), 139.6 (m), 135.0 (s), 132.0 (m), 130.6 (d, $^1J_{P\text{-}C}$ = 17 Hz), 130.5 (s), 129.1 (q, $^2J_{F\text{-}C}$ = 31 Hz), 128.5 (s), 124.7 (q, $^1J_{F\text{-}C}$ = 273 Hz), 117.6 (s), 31.1 (s), 19.7 (s), 19.2 (s). ^{19}F{^{1}H} NMR (CH_2Cl_2, δ): -61.3 (s). ^{31}P{^{1}H} NMR (CD_2Cl_2, δ): 102.3 (s, $^1J_{Pt\text{-}P}$ = 2914 Hz). ^{195}Pt NMR (CD_2Cl_2, δ): -2818 (q, $^1J_{Pt\text{-}P}$ = 2921 Hz). Anal. Calcd. for $C_{68}H_{66}SiP_3PtBF_{24}$: C, 49.02; H, 4.00. Found: C, 48.52; H, 3.60.

Preparation of {[SiP$^{i\mathrm{Pr}}_3$]Pt(H$_2$)}{BAr$^F_4$} (11a). Under a dinitrogen atmosphere, {[SiP$^{i\mathrm{Pr}}_3$]Pt}{BAr$^F_4$} (19 mg, 11 μmol) was dissolved in CD_2Cl_2 and transferred to a J. Young tube. The sample was freeze-pump-thawed three times, then exposed to one atm H_2 while frozen. Upon thawing in the sealed tube, the solution gradually turned pale pink. Unsealing or diluting the sample results in gradual recovery of the four-coordinate starting material's color. ^{1}H NMR (CH_2Cl_2, δ): 8.06 (d, J = 8.1 Hz, 3H), 7.72 (m, 8H, *o*-BAr$^F_4$), 7.56 (m, 4H, *p*-BAr$^F_4$), 7.52 (m, 6H), 7.43 (t, J = 7.1 Hz, 3H), 2.36 (m, 6H), 0.97 (m, 18H), 0.46 (br s, 18H), -1.09 (br s, 2H). ^{1}H NMR (-70 °C, CH_2Cl_2, δ): 8.02 (d, 7.0 Hz), 7.73 (br s, 8H, *o*-BAr$^F_4$), 7.54 (br s, 4H, *p*-BAr$^F_4$), 7.47 (t, J = 7.3 Hz, 6H), 7.38 (t, J = 7.3 Hz, 3H), 2.48 (br s, 3H), 1.99 (br s, 3H), 1.01 (s, 9H), 0.91 (s, 9H), 0.82 (s, 9H), -0.50 (s, 9H), -2.40 (br s, $^1J_{Pt\text{-}H}$ = 264 Hz, 2H). $T_{1(min)}$ (500 MHz, -50 °C) = 26 ms. ^{13}C{^{1}H} NMR (CH_2Cl_2, δ): 162.3 (q, $^1J_{B\text{-}C}$ = 49 Hz), 149.6 (m), 139.3 (m), 135.4 (s), 134.1 (s), 131.8 (s), 130.6 (s), 129.6 (s), 129.4 (q, $^2J_{F\text{-}C}$ = 30 Hz), 125.2 (q, $^1J_{F\text{-}C}$ = 271 Hz), 118.0 (s), 27.5 (s), 18.6 (s). ^{19}F{^{1}H} NMR (CH_2Cl_2, δ): -61.4 (s). ^{31}P{^{1}H} NMR (CH_2Cl_2, δ): 52.4 (s, $^1J_{Pt\text{-}P}$ = 2766 Hz).

Preparation of {[SiP$^{i\mathrm{Pr}}_3$]Pt(HD)}{BAr$^{\mathrm{F}}_4$} (11b). A sample of {[SiP$^{i\mathrm{Pr}}_3$]Pt}{BAr$^{\mathrm{F}}_4$} (19 mg, 11 μmol) dissolved in CD_2Cl_2 in a J. Young tube was freeze-pump-thawed four times, then exposed to ca. 0.4 atm HD (generated from the reaction of excess $LiAlH_4$ and D_2O). Upon thawing in the sealed tube, the solution gradually turned pale pink. ^{1}H NMR (CH_2Cl_2, δ): 8.06 (m, 3H), 7.73 (m, 8H, *o*-BAr$^{\mathrm{F}}_4$), 7.56 (m, 4H, *p*-BAr$^{\mathrm{F}}_4$), 7.52 (m, 6H), 7.43 (t, J = 7.5 Hz, 3H), 2.37 (m, 6H), 0.98 (m, 18H), 0.48 (m, 18H), -1.37 (br t, $^1J_{\mathrm{H\text{-}D}}$ = 33 Hz, 1H). ^{1}H NMR (-70 °C, CH_2Cl_2, δ): 8.02 (d, J = 7.0 Hz, 3H), 7.73 (br s, 8H, *o*-BAr$^{\mathrm{F}}_4$), 7.53 (br s, 4H, *p*-BAr$^{\mathrm{F}}_4$), 7.47 (t, J = 6.7 Hz, 6H), 7.38 (t, J = 6.7 Hz, 3H), 2.48 (br s, 3H), 1.99 (br s, 3H), 1.01 (s, 9H), 0.91 (m, 9H), 0.82 (s, 9H), -0.50 (s, 9H), -2.42 (t, $^1J_{\mathrm{H\text{-}D}}$ = 29 Hz, $^1J_{\mathrm{Pt\text{-}H}}$ = 258 Hz, 1H). ^{13}C{^{1}H} NMR (CH_2Cl_2, δ): 162.3 (q, $^1J_{\mathrm{B\text{-}C}}$ = 49 Hz), 149.7 (m), 139.1 (m), 135.4 (s), 134.1 (s), 131.8 (s), 130.6 (m), 130.0, (m), 129.4 (q, $^2J_{\mathrm{C\text{-}F}}$ = 32 Hz), 250.4 (q, $^1J_{\mathrm{C\text{-}F}}$ = 273 Hz), 118.0 (s), 27.6 (s), 18.6 (s). ^{19}F{^{1}H} NMR (CH_2Cl_2, δ): -61.2 (s). ^{31}P{^{1}H} NMR (CH_2Cl_2, δ): 52.4 (s, $^1J_{\mathrm{Pt\text{-}P}}$ = 2765 Hz).

Deprotonation of {[SiP$^{i\mathrm{Pr}}_3$]Pt(H$_2$)}{BAr$^{\mathrm{F}}_4$} by 2,6-lutidine. Under a dinitrogen atmosphere, {[SiP$^{i\mathrm{Pr}}_3$]Pt}{BAr$^{\mathrm{F}}_4$} (5 mg, 3 μmol) was dissolved in CD_2Cl_2 in a J. Young tube to form a purple solution. One drop of 2,6-lutidine was added with no visible color change. The ^{1}H and 31P NMR spectra of the resulting solution retained the resonances of the starting material, over which the resonances of 2,6-lutidine ((CH_2Cl_2, δ): 7.45 (t, J = 7.6 Hz, 1H), 6.94 (d, J = 7.6 Hz, 2H), 2.46 (s, 6H)) were superimposed. The sample was freeze-pump-thawed once, then exposed to one atm of H_2, resulting in a pale pink solution. The ^{1}H and ^{31}P NMR spectra revealed the characteristic resonances of both {[SiP$^{i\mathrm{Pr}}_3$]Pt(H$_2$)}{BAr$^{\mathrm{F}}_4$} and [SiP$^{i\mathrm{Pr}}_3$]Pt-H at a ratio of approximately 2.3:1 after six days at room temperature in the sealed tube.

Preparation of {[SiP$^{i\mathrm{Pr}}_3$]Pt(NCMe)}{BAr$^{\mathrm{F}}_4$} (12). Under a dinitrogen atmosphere, purple crystals of {[SiP$^{i\mathrm{Pr}}_3$]Pt}{BAr$^{\mathrm{F}}_4$} (15 mg, 9 μmol) were added to a J. Young tube. 0.5 mL of a 17 mM solution of MeCN in CD_2Cl_2 (9 μmol) was added to the tube, which was sealed and shaken, resulting in a colorless solution. Volatiles were removed to yield a white soild. Colorless crystals suitable for X-ray diffraction were grown by slow diffusion of pentane vapors into a CH_2Cl_2 solution. ^{1}H NMR (CH_2Cl_2, δ): 7.96 (m, 3H), 7.74 (m, 8H, *o*-BAr$^{\mathrm{F}}_4$), 7.57 (m, 4H, *p*-BAr$^{\mathrm{F}}_4$), 7.49 (m, 3H), 7.39 (m, 6H), 2.68 (m, 6H), 2.39 (s, 3H, Pt-NCC*H*$_3$), 1.10 (m, 18H), 0.54 (m, 18H). ^{13}C{^{1}H} NMR (CH_2Cl_2, δ): 161.9 (q, $^1J_{\mathrm{B\text{-}C}}$ = 50 Hz), 149.4 (m), 139.6 (m), 134.9 (s), 133.1 (m), 130.4 (s), 129.6 (m), 129.2 (s), 128.8 (m), 127.4 (m, Pt-N*C*CH$_3$), 124.7 (q, $^1J_{\mathrm{F\text{-}C}}$ = 273 Hz), 117.6 (s), 27.9 (s), 18.4 (s), 17.9 (s), 3.8 (s, Pt-NC*C*H$_3$). ^{19}F{^{1}H} NMR (CH_2Cl_2, δ): -61.3 (s). ^{31}P{^{1}H} NMR (CH_2Cl_2, δ): 43.9 (s, $^1J_{\mathrm{Pt\text{-}P}}$ = 2950 Hz). Anal. Calcd. for $C_{70}H_{69}SiP_3PtNBF_{24}$: C, 49.23; H, 4.07. Found: C, 49.34; H, 4.08.

Preparation of {[SiP$^{i\mathrm{Pr}}_3$]Pt(pyridine)}{BAr$^{\mathrm{F}}_4$} (13). Under a dinitrogen atmosphere, {[SiP$^{i\mathrm{Pr}}_3$]Pt}{BAr$^{\mathrm{F}}_4$} (15 mg, 9 μmol) was dissolved in CD_2Cl_2 containing 5 equiv pyridine (3.5 mg, 45 μmol), resulting in a colorless solution. Colorless crystals suitable for X-ray diffraction were grown by diffusion of pentane vapors into a CH_2Cl_2 solution. The room temperature solution spectra were consistent with a three-fold symmetric species, suggesting a rapid equilibrium between the square-planar pyridine adduct seen in the solid-state structure and the trigonal pyramidal, four-coordinate starting material; dilution of the sample results in gradual recovery of the starting material's color. ^{1}H NMR (CH_2Cl_2, δ): 8.68 (s, 3H), 8.65 (m, 2H, pyr), 7.73 (m, 9H, *o*-BAr$^{\mathrm{F}}_4$ + pyr), 7.56 (s, 4H, *p*-BAr$^{\mathrm{F}}_4$), 7.48 (t, J = 6.9 Hz, 6H), 7.39 (t, J = 7.2 Hz, 3H), 7.36 (m, 2H, pyr). ^{13}C{^{1}H} NMR (CH_2Cl_2, δ): 140.9 (m), 138.0 (m), 138.7 (s), 131.6 (s),

130.0 (m), 128.9 (s), 27.4 (s), 19.7 (s), 19.1 (s). $^{19}F\{^{1}H\}$ NMR (CH_2Cl_2, δ): -61.2 (s). $^{31}P\{^{1}H\}$ NMR (CH_2Cl_2, δ): 39.9 (v br).

Preparation of [SiP$^{i\text{Pr}}_3$]Pd-CH$_3$ (14). Under a dinitrogen atmosphere, [SiP$^{i\text{Pr}}_3$]Pd-Cl (16 mg, 22 μmol) was dissolved in Et_2O and cooled to -78 °C. MeLi in Et_2O (4.1 mL of 0.16M solution, 66 μmol) was added dropwise at -78 °C. The resulting faintly colored solution was allowed to warm to room temperature overnight, then stirred at room temperature for 1 hr. Volatiles were removed to yield an off-white solid, which was dissolved in pentane and filtered through Celite. Volatiles were removed again, and the resulting white solids washed with MeCN to afford spectroscopically and analytically pure [SiP$^{i\text{Pr}}_3$]Pd-CH_3 (15 mg, 94%). ^{1}H NMR (C_6D_6, δ): 8.05 (m, 3H), 7.22 (t, J = 7.8 Hz, 6H), 7.05 (t, J = 7.2 Hz, 3H), 2.41 (sept, J = 6.3 Hz, 6H), 1.06 (m, 18H), 0.64 (m, 18H), 0.60 (q, J = 6.9Hz, 3H, Pd-CH_3). $^{13}C\{^{1}H\}$ NMR (C_6D_6, δ): 156.1 (m), 146.2 (m), 134.1 (m), 130.1 (s), 129.1 (s), 127.3 (s), 27.6 (m), 19.0 (s), 18.5 (s), -27.2 (q, $^{2}J_{P\text{-}C}$ = 12.7 Hz, Pd-CH$_3$). $^{31}P\{^{1}H\}$ NMR (C_6D_6, δ): 45.2 (s). Anal. Calcd. for $C_{37}H_{57}SiP_3Pd$: C, 60.94; H, 7.88. Found: C, 59.96; H, 7.67.

Preparation of [SiP$^{i\text{Pr}}_3$]Pd-Cl (15). Under a dinitrogen atmosphere, [SiP$^{i\text{Pr}}_3$]H (60 mg, 99 μmol) and (COD)PdMeCl (31 mg, 117 μmol) were weighed out into a vial. Approximately 3 mL C_6H_6 were added and resulted in an immediate color change to a yellow solution and release of CH_4 bubbles. The solution was stirred at room temperature overnight. Volatiles were removed and the residue was dissolved in C_6H_6 and filtered though Celite. Volatiles were removed again and the remaining solid was washed liberally with pentane to afford [SiP$^{i\text{Pr}}_3$]Pd-Cl as a yellow powder (66 mg, 89%). Analytically pure material and crystals suitable for X-ray diffraction were grown by slow diffusion of pentane into a CH_2Cl_2 solution of [SiP$^{i\text{Pr}}_3$]Pd-CH_3, which converts to [SiP$^{i\text{Pr}}_3$]PdCl upon prolonged exposure to CH_2Cl_2. ^{1}H NMR (CD_2Cl_2, δ): 7.87-7.84 (m, 3H), 7.51-7.49 (m, 3H), 7.38-7.30 (m, 6H), 2.51 (sept, J = 6.9 Hz, 6H), 1.13 (m, 18H), 0.72 (m, 18H). $^{13}C\{^{1}H\}$ NMR (CD_2Cl_2, δ): 153.4 (m), 141.8 (m), 134.0 (m), 130.7 (s), 129.7 (s), 128.8 (s), 26.8 (s), 18.6 (s), 18.4 (s). $^{31}P\{^{1}H\}$ NMR (CD_2Cl_2, δ): 42.2 (s). Anal. Calcd. for $C_{36}H_{54}SiP_3PdCl$: C, 57.68; H, 7.26. Found: C, 57.98; H, 7.07.

Preparation of {[SiP$^{i\text{Pr}}_3$]Pd}{BAr$^{F}_4$} (16). Under a dinitrogen atmosphere, [SiP$^{i\text{Pr}}_3$]Pd-CH_3 (10 mg, 13 μmol) and HBAr$^{F}_4$•2Et_2O (13 mg, 13 μmol) were dissolved in CH_2Cl_2, resulting in an immediate color change to a purple-red solution and release of CH_4 bubbles. Pentane vapors were diffused into a CH_2Cl_2 solution at -35 °C to afford {[SiP$^{i\text{Pr}}_3$]Pd}{BAr$^{F}_4$} as a purple-red solid, which was dried under vacuum (19 mg, 88%). Analytically pure material was obtained by crystallization by layering pentane over a CH_2Cl_2 solution at -35 °C. Crystals suitable for X-ray diffraction were grown by slow diffusion of pentane into a CH_2Cl_2 solution. ^{1}H NMR (CD_2Cl_2, δ): 7.72 (m, 11H, 8H from o-BAr$^{F}_4$), 7.69-7.62 (m, 6H), 7.56 (s, 4H, p-BAr$^{F}_4$), 7.52-7.47 (m, 3H), 2.67 (m, 6H), 1.07 (m, 18H), 0.90 (m, 18H). $^{13}C\{^{1}H\}$ NMR (CH_2Cl_2, δ): 162.3 (q, $^{1}J_{B\text{-}C}$ = 50 Hz), 148 5 (m), 138.7 (m), 135.4 (s), 133.7 (m), 131.5 (d, $^{1}J_{P\text{-}C}$ = 18 Hz), 131.0 (s), 129.4 (q, $^{2}J_{F\text{-}C}$ = 32 Hz), 129.1 (s), 125.2 (q, $^{1}J_{F\text{-}C}$ = 273 Hz), 118.0 (s), 27.6 (s), 19.9 (s), 19.3 (s). $^{19}F\{^{1}H\}$ NMR (CD_2Cl_2, δ): -61.3 (s). $^{31}P\{^{1}H\}$ NMR (CD_2Cl_2, δ): 53.6 (s). Anal. Calcd. for. $C_{68}H_{66}SiP_3PdBF_{24}$: C, 51.78; H, 4.22. Found: C, 51.23; H, 4.16.

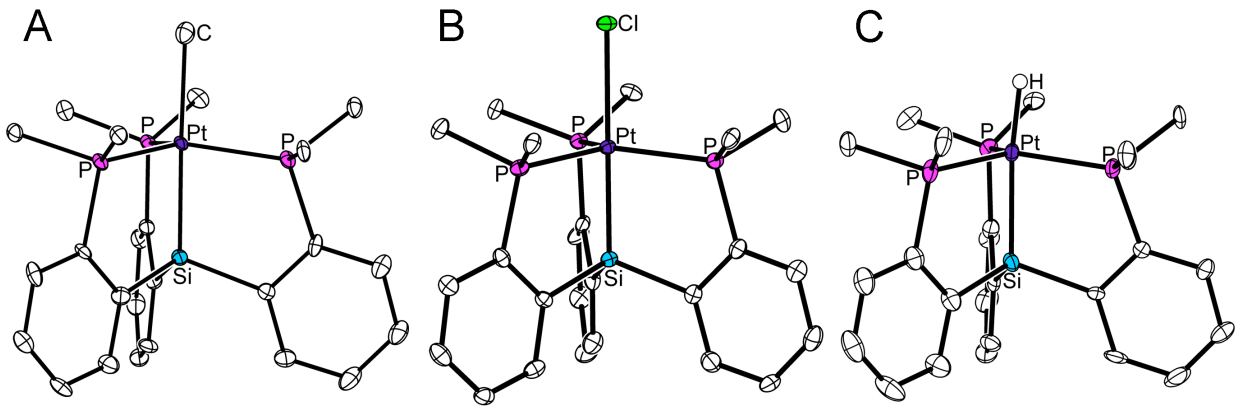

Figure S1. Solid-state structures of (A) **1**, (B) **2**, and (C) **3**. Thermal ellipsoids drawn at 50% probability. Hydrogen atoms and solvent molecules omitted for clarity. [SiP^{Ph}_3] ligand -PPh_2 rings abbreviated to show only the ipso C-atom of each ring.

Table S1a. Crystal data and structure refinement for **1**.

Identification code	npm74	
Empirical formula	C63 H61 O2 P3 Pt Si	
Formula weight	1166.21	
Temperature	100(2) K	
Wavelength	0.71073 Å	
Crystal system	Monoclinic	
Space group	P2(1)/c	
Unit cell dimensions	a = 18.745(2) Å	α = 90°.
	b = 16.1454(18) Å	β = 94.181(4)°.
	c = 16.911(2) Å	γ = 90°.
Volume	5104.4(10) $Å^3$	
Z	4	
Density (calculated)	1.518 Mg/m^3	
Absorption coefficient	2.913 mm^{-1}	
F(000)	2368	
Crystal size	0.30 x 0.08 x 0.05 mm^3	
Theta range for data collection	1.67 to 29.13°.	
Index ranges	-25<=h<=24, -21<=k<=22, -23<=l<=21	
Reflections collected	75418	
Independent reflections	13406 [R(int) = 0.1465]	
Completeness to theta = 29.13°	97.7 %	
Absorption correction	Semi-empirical from equivalents	
Max. and min. transmission	0.8680 and 0.4753	

Refinement method	Full-matrix least-squares on F^2
Data / restraints / parameters	13406 / 613 / 632
Goodness-of-fit on F^2	1.091
Final R indices [I>2sigma(I)]	R1 = 0.0506, wR2 = 0.1189
R indices (all data)	R1 = 0.0844, wR2 = 0.1457
Largest diff. peak and hole	5.837 and -2.011 e.Å^{-3}

Table S1b. Selected bond lengths [Å] and angles [°] for **1**.

Pt(1)-C(100)	2.229(6)
Pt(1)-Si(1)	2.3076(15)
Pt(1)-P(1)	2.3034(14)
Pt(1)-P(2)	2.3038(14)
Pt(1)-P(3)	2.3229(14)

C(100)-Pt(1)-Si(1)	178.15(16)
P(1)-Pt(1)-P(2)	125.74(5)
P(1)-Pt(1)-P(3)	113.77(5)
P(2)-Pt(1)-P(3)	117.56(5)
C(100)-Pt(1)-P(1)	94.70(15)
C(100)-Pt(1)-P(2)	94.89(17)
C(100)-Pt(1)-P(3)	97.66(16)
P(1)-Pt(1)-Si(1)	84.39(5)
P(2)-Pt(1)-Si(1)	84.36(5)
P(3)-Pt(1)- Si(1)	84.18(5)

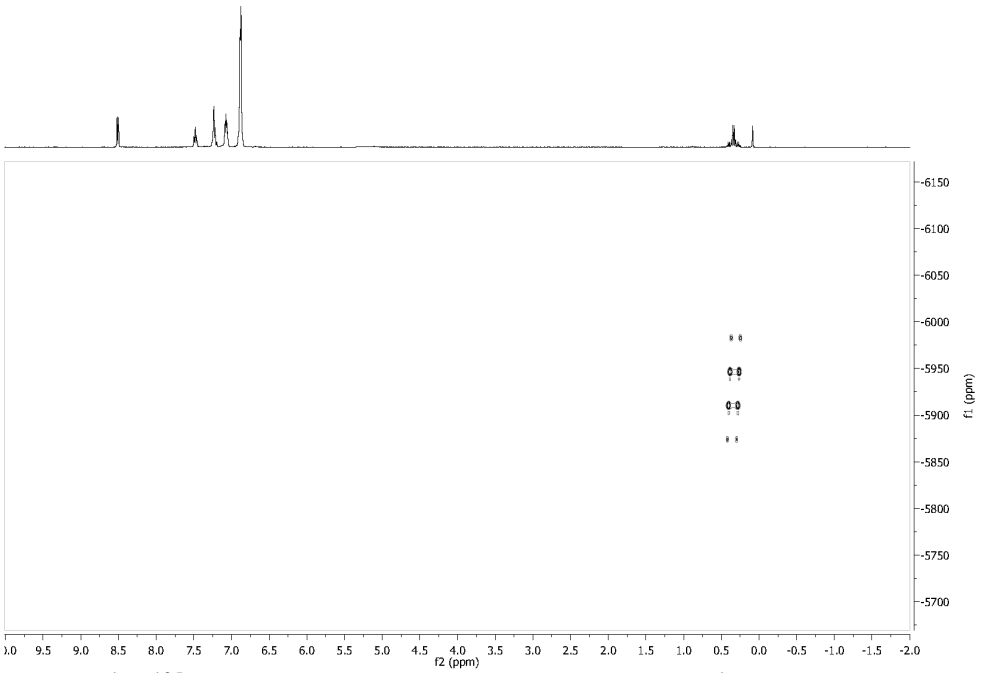

Figure S2. $^{1}H/^{195}Pt$ 2D HMBC NMR spectrum of **1**. ^{1}H NMR resonances along horizontal axis (f2) and ^{195}Pt NMR resonances along vertical axis (f1).

Table S2a. Crystal data and structure refinement for **2**.

Identification code	npm75	
Empirical formula	C55 H44 Cl3 P3 Pt Si	
Formula weight	1127.34	
Temperature	100(2) K	
Wavelength	0.71073 Å	
Crystal system	Triclinic	
Space group	P-1	
Unit cell dimensions	a = 11.1768(12) Å	α = 87.699(2)°.
	b = 13.3695(14) Å	β = 84.961(2)°.
	c = 15.7387(16) Å	γ = 86.359(2)°.
Volume	2336.6(4) $Å^3$	
Z	2	
Density (calculated)	1.602 Mg/m^3	
Absorption coefficient	3.341 mm^{-1}	
F(000)	1124	
Crystal size	0.19 x 0.10 x 0.08 mm^3	
Theta range for data collection	1.53 to 29.15°.	
Index ranges	-15<=h<=14, -17<=k<=17, -20<=l<=21	

Reflections collected	40452
Independent reflections	11408 [R(int) = 0.0562]
Completeness to theta = 25.00°	99.7 %
Absorption correction	Semi-empirical from equivalents
Max. and min. transmission	0.7759 and 0.5693
Refinement method	Full-matrix least-squares on F^2
Data / restraints / parameters	11408 / 510 / 568
Goodness-of-fit on F^2	1.082
Final R indices [I>2sigma(I)]	R1 = 0.0422, wR2 = 0.1040
R indices (all data)	R1 = 0.0489, wR2 = 0.1081
Largest diff. peak and hole	3.382 and -2.062 e.Å^{-3}

Table S2b. Selected bond lengths [Å] and angles [°] for **2**.

Pt(1)-Cl(1)	2.4975(10)
Pt(1)-Si	2.2689(11)
Pt(1)-P(1)	2.3173(11)
Pt(1)-P(2)	2.3530(11)
Pt(1)-P(3)	2.3177(10)

Cl(1)-Pt(1)- Si	178.17(3)
P(1)-Pt(1)-P(2)	117.20(4)
P(1)-Pt(1)-P(3)	125.31(4)
P(3)-Pt(1)-P(2)	115.63(4)
P(1)-Pt(1)-Cl(1)	95.02(4)
P(2)-Pt(1)-Cl(1)	95.99(4)
P(3)-Pt(1)-Cl(1)	92.68(3)
Si-Pt(1)-P(1)	85.28(4)
Si-Pt(1)-P(2)	85.46(4)
Si-Pt(1)-P(3)	85.68(4)

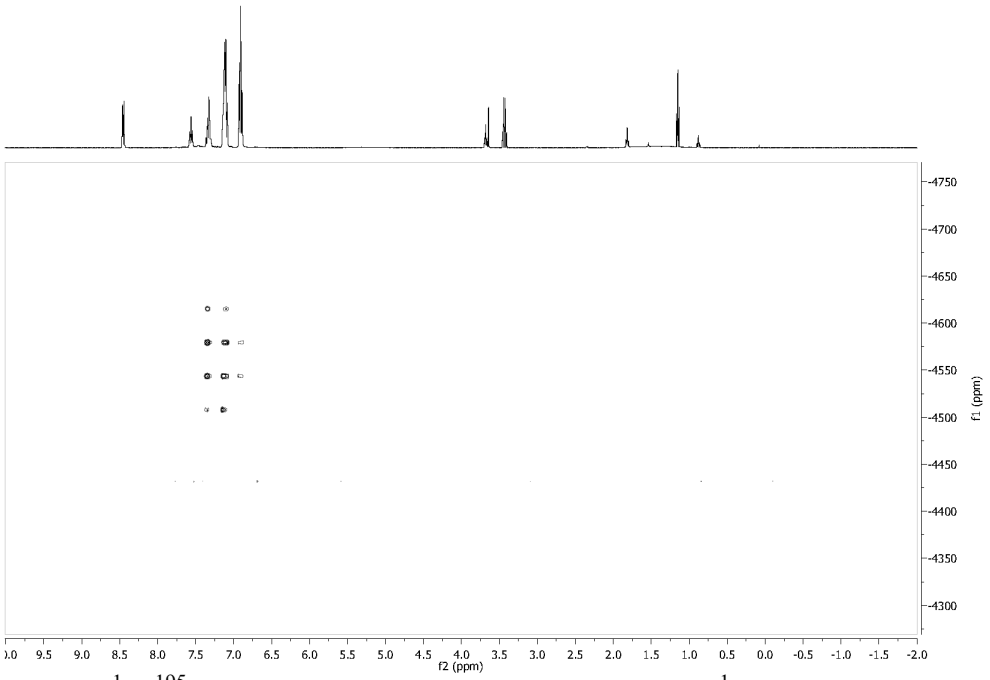

Figure S3. $^{1}H/^{195}Pt$ 2D HMBC NMR spectrum of **2**. ^{1}H NMR resonances along horizontal axis (f2) and ^{195}Pt NMR resonances along vertical axis (f1).

Table S3a. Crystal data and structure refinement for **3**.

Identification code	npm78	
Empirical formula	C62 H59 O2 P3 Pt Si	
Formula weight	1152.18	
Temperature	100(2) K	
Wavelength	0.71073 Å	
Crystal system	Monoclinic	
Space group	P2(1)/c	
Unit cell dimensions	a = 18.572(3) Å	α = 90°.
	b = 16.157(3) Å	β = 96.473(3)°.
	c = 16.968(3) Å	γ = 90°.
Volume	5059.0(15) $Å^3$	
Z	4	
Density (calculated)	1.513 Mg/m^3	
Absorption coefficient	2.938 mm^{-1}	
F(000)	2336	
Crystal size	0.19 x 0.07 x 0.07 mm^3	
Theta range for data collection	1.10 to 28.70°.	
Index ranges	-24<=h<=22, -21<=k<=19, -22<=l<=22	

Reflections collected	30622
Independent reflections	11907 [R(int) = 0.0651]
Completeness to theta = 25.00°	99.3 %
Absorption correction	Semi-empirical from equivalents
Max. and min. transmission	0.8208 and 0.6052
Refinement method	Full-matrix least-squares on F^2
Data / restraints / parameters	11907 / 1626 / 892
Goodness-of-fit on F^2	1.025
Final R indices [I>2sigma(I)]	R1 = 0.0435, wR2 = 0.0872
R indices (all data)	R1 = 0.0776, wR2 = 0.1036
Largest diff. peak and hole	2.286 and -1.608 e.Å^{-3}

Table S3b. Selected bond lengths [Å] and angles [°] for **3**.

Pt(1)-Si(1)	2.3134(13)
Pt(1)-P(1)	2.3061(13)
Pt(1)-P(2)	2.2947(13)
Pt(1)-P(3)	2.3001(11)

P(1)-Pt(1)-P(2)	119.05(4)
P(1)-Pt(1)- P(3)	114.37(4)
P(2)-Pt(1)-P(3)	124.19(4)
P(1)-Pt(1)-Si(1)	84.94(5)
P(2)-Pt(1)-Si(1)	84.79(5)
P(3)-Pt(1)-Si(1)	84.83(4)

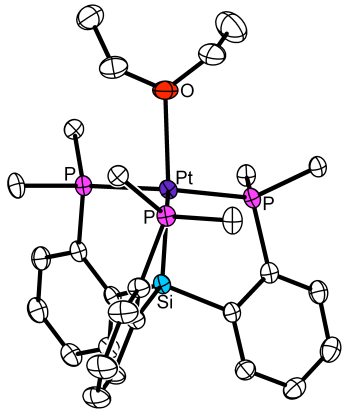

Figure S4. Solid-state structure of **4**. Thermal ellipsoids drawn at 50% probability. Hydrogen atoms, solvent molecules, and BAr^F_4 anion omitted for clarity. [SiP^{Ph}_3] ligand - PPh_2 rings abbreviated to show only the ipso C-atom of each ring.

Table S4a. Crystal data and structure refinement for **4**.

Identification code	08236	
Empirical formula	C90 H64 B F24 O P3 Pt Si	
Formula weight	1944.31	
Temperature	100(2) K	
Wavelength	0.71073 Å	
Crystal system	Triclinic	
Space group	P-1	
Unit cell dimensions	a = 13.1515(15) Å	α = 65.549(2)°.
	b = 17.621(2) Å	β = 77.723(2)°.
	c = 19.654(2) Å	γ = 86.737(2)°.
Volume	4049.0(8) $Å^3$	
Z	2	
Density (calculated)	1.595 Mg/m^3	
Absorption coefficient	1.911 mm^{-1}	
F(000)	1940	
Crystal size	0.15 x 0.15 x 0.10 mm^3	
Theta range for data collection	1.16 to 28.28°.	
Index ranges	-17<=h<=17, -23<=k<=23, -26<=l<=26	
Reflections collected	99238	
Independent reflections	20105 [R(int) = 0.0817]	
Completeness to theta = 28.28°	99.9 %	
Absorption correction	Semi-empirical from equivalents	
Max. and min. transmission	0.8319 and 0.7625	
Refinement method	Full-matrix least-squares on F^2	
Data / restraints / parameters	20105 / 2145 / 1112	
Goodness-of-fit on F^2	1.037	
Final R indices [I>2sigma(I)]	R1 = 0.0463, wR2 = 0.1053	
R indices (all data)	R1 = 0.0663, wR2 = 0.1152	
Largest diff. peak and hole	3.132 and -1.226 $e.Å^{-3}$	

Table S4b. Selected bond lengths [Å] and angles [°] for **4**.

Pt(1)-O(1)	2.391(3)
Pt(1)-Si(1)	2.2739(12)
Pt(1)-P(1)	2.3581(11)

Pt(1)-P(2)	2.3761(11)
Pt(1)-P(3)	2.3913(11)

Si(1)-Pt(1)-O(1)	174.06(9)
P(1)-Pt(1)-P(2)	119.94(4)
P(1)-Pt(1)-P(3)	121.38(4)
P(2)-Pt(1)-P(3)	115.12(4)
O(1)-Pt(1)- P(1)	93.86(9)
O(1)-Pt(1)- P(2)	92.45(9)
O(1)-Pt(1)-P(3)	102.57(9)
Si(1)-Pt(1)-P(1)	83.79(4)
Si(1)-Pt(1)-P(2)	84.05(4)
Si(1)-Pt(1)-P(3)	83.28(4)

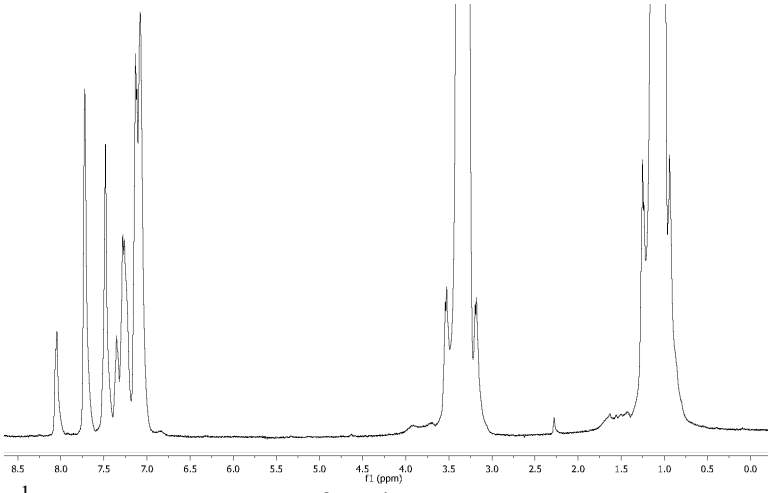

Figure S5a. ^{1}H NMR spectrum of **4** in Et_2O at room temperature; large upfield resonances are from the Et_2O solvent.

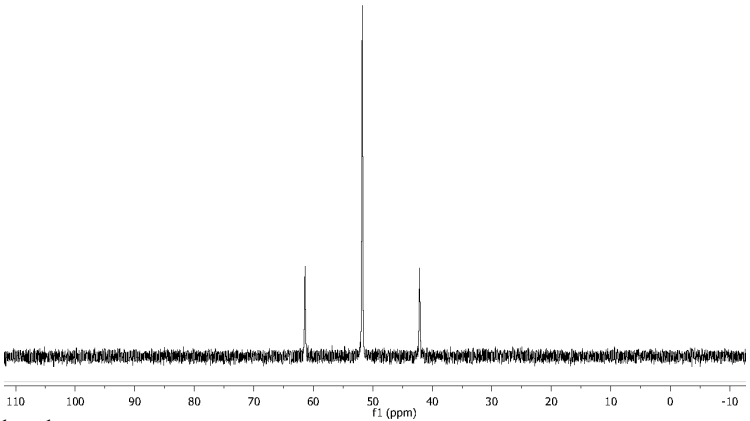

Figure S5b. $^{31}P\{^{1}H\}$ NMR spectrum of **4** in Et_2O at room temperature.

Table S5a. Crystal data and structure refinement for **5**.

Identification code	npm83	
Empirical formula	C45 H31 B0.50 Cl4 F12 P1.50 Pt0.50 Si0.50	
Formula weight	1104.95	
Temperature	100(2) K	
Wavelength	0.71073 Å	
Crystal system	Triclinic	
Space group	P-1	
Unit cell dimensions	a = 12.6057(11) Å	α = 84.459(2)°.
	b = 17.5913(16) Å	β = 84.435(2)°.
	c = 20.2306(18) Å	γ = 86.795(2)°.
Volume	4439.2(7) $Å^3$	
Z	4	
Density (calculated)	1.653 Mg/m^3	
Absorption coefficient	1.986 mm^{-1}	
F(000)	2192	
Crystal size	0.38 x 0.09 x 0.05 mm^3	
Theta range for data collection	1.61 to 27.87°.	
Index ranges	-15<=h<=16, -23<=k<=23, -26<=l<=25	
Reflections collected	54713	
Independent reflections	19579 [R(int) = 0.0645]	
Completeness to theta = 25.00°	99.6 %	
Absorption correction	Semi-empirical from equivalents	
Max. and min. transmission	0.9072 and 0.5191	
Refinement method	Full-matrix least-squares on F^2	
Data / restraints / parameters	19579 / 1727 / 1163	
Goodness-of-fit on F^2	1.050	
Final R indices [I>2sigma(I)]	R1 = 0.0635, wR2 = 0.1600	
R indices (all data)	R1 = 0.0840, wR2 = 0.1736	
Largest diff. peak and hole	3.246 and -2.506 $e.Å^{-3}$	

Table S5b. Selected bond lengths [Å] and angles [°] for **5**.

Pt(1)-Cl(11)	2.6236(16)
Pt(1)-Si(1)	2.2805(16)
Pt(1)-P(1)	2.3321(15)

Pt(1)-P(2)	2.3553(14)
Pt(1)-P(3)	2.3400(15)

Si(1)-Pt(1)-Cl(11)	174.48(5)
P(1)-Pt(1)-P(2)	120.85(5)
P(1)-Pt(1)-P(3)	119.36(5)
P(3)-Pt(1)-P(2)	116.48(5)
P(1)-Pt(1)-Cl(11)	93.60(5)
P(2)-Pt(1)-Cl(11)	94.26(5)
P(3)-Pt(1)-Cl(11)	100.43(5)
Si(1)-Pt(1)-P(1)	82.21(5)
Si(1)-Pt(1)-P(2)	84.88(5)
Si(1)-Pt(1)-P(3)	84.80(6)

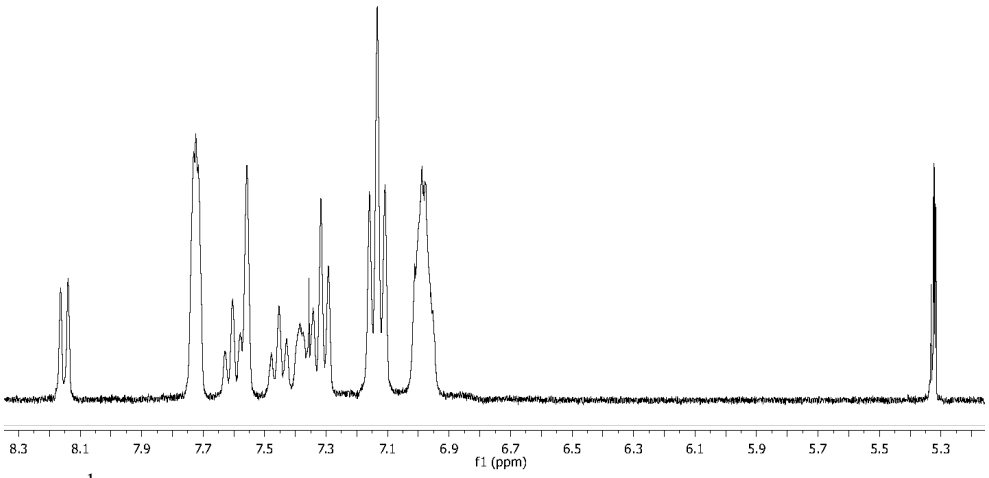

Figure S6a. ^{1}H NMR spectrum of **5** in CD_2Cl_2 at room temperature; **5** has no resonances further upfield.

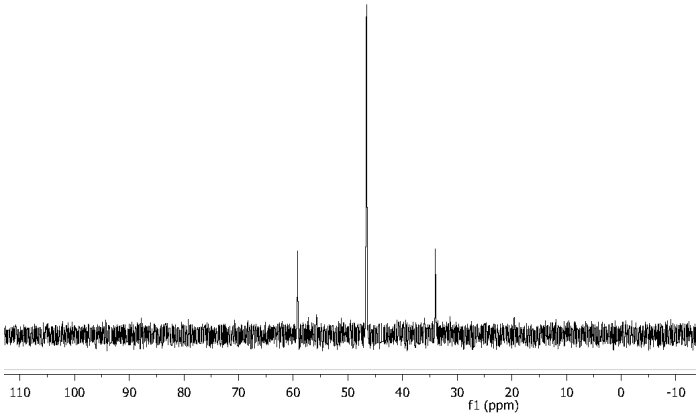

Figure S6b. $^{31}P\{^{1}H\}$ NMR spectrum of **5** in CD_2Cl_2 at room temperature.

Table S6a. Crystal data and structure refinement for **6**.

Identification code	08350	
Empirical formula	C46.50 H29.50 B0.50 F12 P1.50 Pt0.50 Si0.50	
Formula weight	979.65	
Temperature	100(2) K	
Wavelength	0.71073 Å	
Crystal system	Triclinic	
Space group	P-1	
Unit cell dimensions	a = 13.2678(11) Å	α = 84.415(2)°.
	b = 17.6132(15) Å	β = 72.421(2)°.
	c = 18.7753(16) Å	γ = 86.3900(10)°.
Volume	4160.2(6) $Å^3$	
Z	4	
Density (calculated)	1.564 Mg/m^3	
Absorption coefficient	1.860 mm^{-1}	
F(000)	1950	
Crystal size	0.33 x 0.25 x 0.14 mm^3	
Theta range for data collection	1.14 to 29.57°.	
Index ranges	-18<=h<=18, -24<=k<=24, -26<=l<=26	
Reflections collected	74144	
Independent reflections	23200 [R(int) = 0.0456]	
Completeness to theta = 29.57°	99.3 %	
Absorption correction	Semi-empirical from equivalents	
Max. and min. transmission	0.7807 and 0.5789	
Refinement method	Full-matrix least-squares on F^2	
Data / restraints / parameters	23200 / 2293 / 1142	
Goodness-of-fit on F^2	1.045	
Final R indices [I>2sigma(I)]	R1 = 0.0351, wR2 = 0.0745	
R indices (all data)	R1 = 0.0448, wR2 = 0.0795	
Largest diff. peak and hole	1.494 and -1.094 $e.Å^{-3}$	

Table S6b. Selected bond lengths [Å] and angles [°] for **6**.

Pt(1)-Si(1)	2.2806(8)
Pt(1)-P(1)	2.3816(7)

Pt(1)-P(2)	2.3754(8)
Pt(1)-P(3)	2.3944(7)
C(11T)-C(12T)	1.509(5)
C(12T)-C(13T)	1.373(5)
C(12T)-C(17T)	1.389(6)
C(13T)-C(14T)	1.378(6)
C(14T)-C(15T)	1.347(7)
C(15T)-C(16T)	1.380(7)
C(16T)-C(17T)	1.381(6)

P(1)-Pt(1)-P(2)	121.50(3)
P(1)-Pt(1)-P(3)	115.94(2)
P(2)-Pt(1)-P(3)	118.55(2)
Si(1)-Pt(1)-P(1)	83.08(3)
Si(1)-Pt(1)-P(2)	83.25(3)
Si(1)-Pt(1)-P(3)	83.62(3)
C(13T)-C(12T)-C(17T)	118.7(3)
C(13T)-C(12T)-C(11T)	120.6(4)
C(17T)-C(12T)-C(11T)	120.7(4)
C(12T)-C(13T)-C(14T)	120.9(4)
C(15T)-C(14T)-C(13T)	120.8(4)
C(14T)-C(15T)-C(16T)	119.3(4)
C(15T)-C(16T)-C(17T)	120.9(4)
C(16T)-C(17T)-C(12T)	119.5(4)

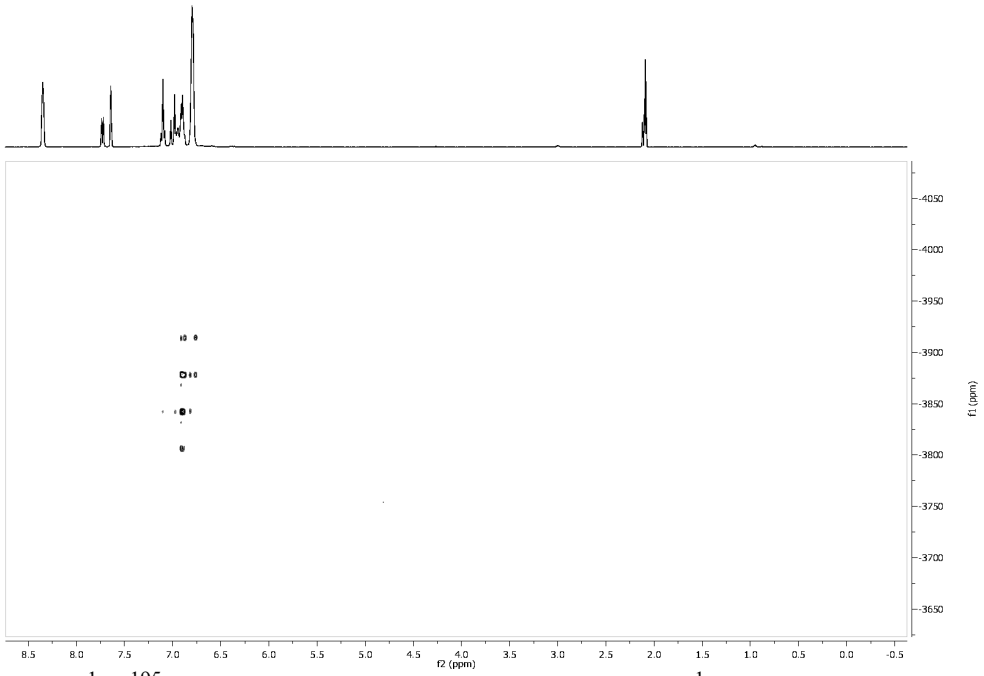

Figure S7. $^{1}H/^{195}Pt$ 2D HMBC NMR spectrum of **6**. ^{1}H NMR resonances along horizontal axis (f2) and ^{195}Pt NMR resonances along vertical axis (f1).

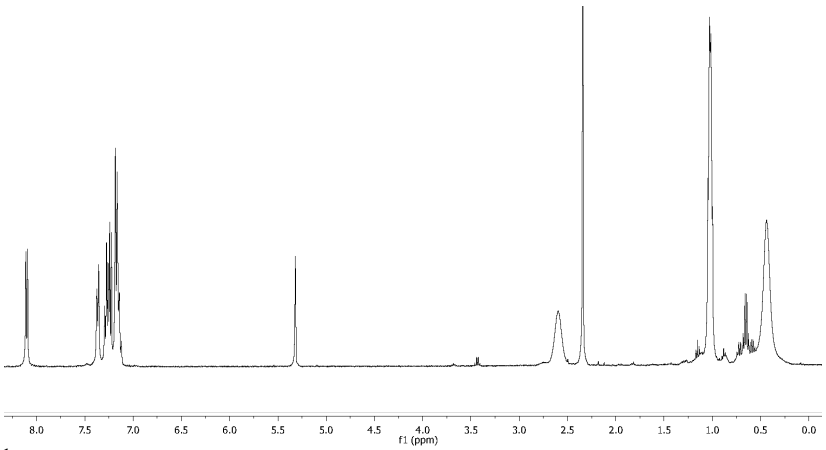

Figure S8a. ^{1}H NMR spectrum of **7** in CD_2Cl_2 at room temperature.

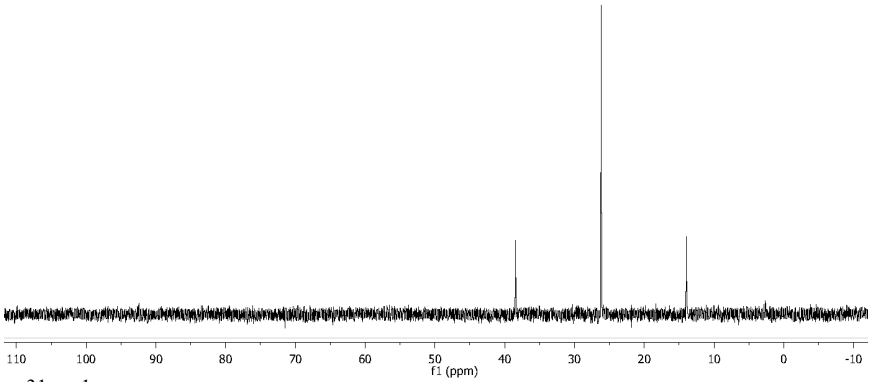

Figure S8b. $^{31}P\{^{1}H\}$ spectrum of **7** in CD_2Cl_2 at room temperature.

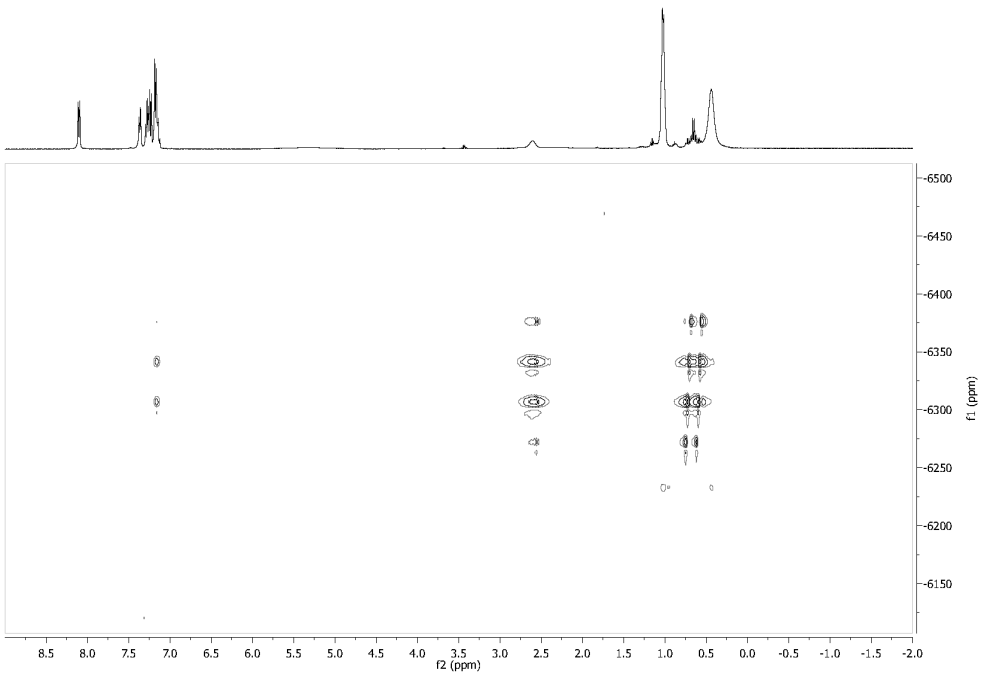

Figure S9. $^{1}H/^{195}Pt$ 2D HMBC NMR spectrum of **7**. ^{1}H NMR resonances along horizontal axis (f2) and ^{195}Pt NMR resonances along vertical axis (f1).

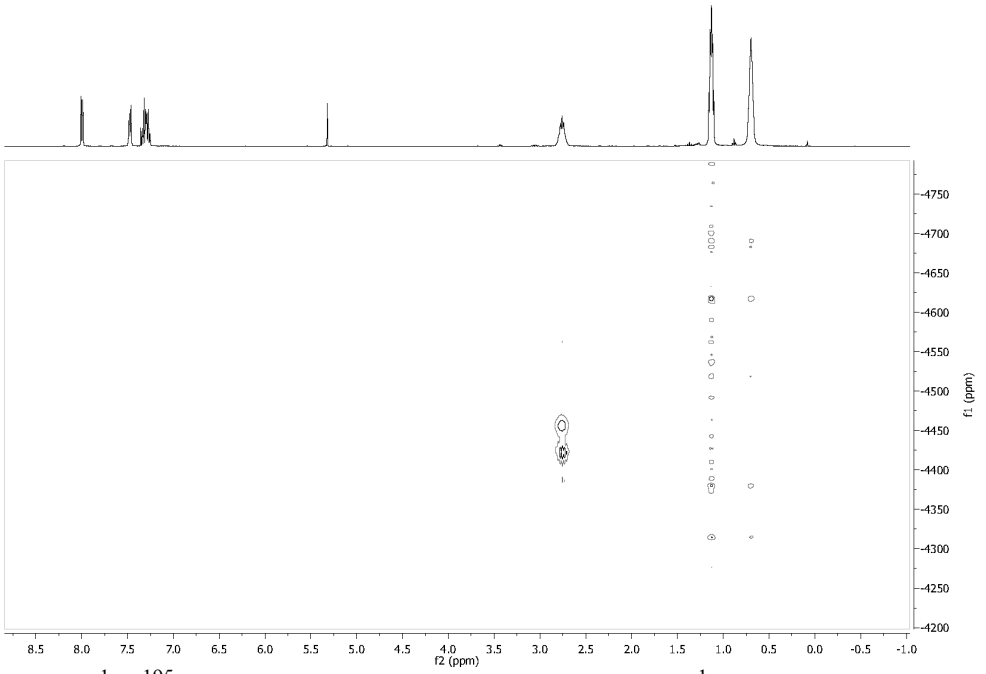

Figure S10. $^{1}H/^{195}Pt$ 2D HMBC NMR spectrum of **8**. ^{1}H NMR resonances along horizontal axis (f2) and ^{195}Pt NMR resonances along vertical axis (f1).

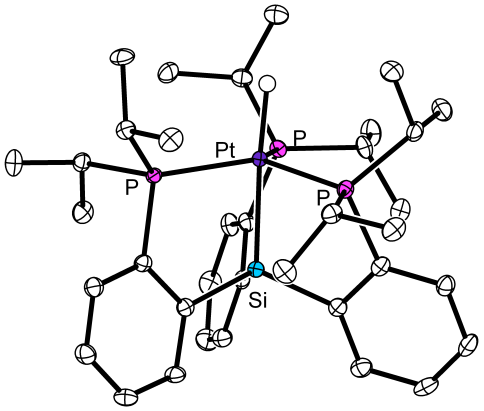

Figure S11. Solid-state structure of **9**. Thermal ellipsoids drawn at **50**% probability. Hydrogen atoms and solvent molecules omitted for clarity.

Table S7a. Crystal data and structure refinement for **9**.

Identification code	08093	
Empirical formula	C38.50 H61 P3 Pt Si	
Formula weight	839.96	
Temperature	100(2) K	
Wavelength	0.71073 Å	
Crystal system	Triclinic	
Space group	P-1	
Unit cell dimensions	a = 11.088(2) Å	α = 89.95(3)°.
	b = 11.156(2) Å	β = 88.84(3)°.
	c = 35.058(7) Å	γ = 61.63(3)°.
Volume	3814.7(13) $Å^3$	
Z	4	
Density (calculated)	1.463 Mg/m^3	
Absorption coefficient	3.861 mm^{-1}	
F(000)	1716	
Crystal size	0.15 x 0.10 x 0.05 mm^3	
Theta range for data collection	0.58 to 30.03°.	
Index ranges	-15<=h<=15, -15<=k<=15, -49<=l<=49	
Reflections collected	105344	
Independent reflections	22260 [R(int) = 0.0534]	
Completeness to theta = 30.03°	99.7 %	
Absorption correction	Semi-empirical from equivalents	
Max. and min. transmission	0.8304 and 0.5951	
Refinement method	Full-matrix least-squares on F^2	

Data / restraints / parameters	22260 / 780 / 834
Goodness-of-fit on F^2	1.062
Final R indices [I>2sigma(I)]	R1 = 0.0307, wR2 = 0.0637
R indices (all data)	R1 = 0.0407, wR2 = 0.0674
Largest diff. peak and hole	1.475 and -1.198 e.Å^{-3}

Table S7b. Selected bond lengths [Å] and angles [°] for **9**.

Pt(1)-Si(1)	2.3116(10)
Pt(1)-P(1)	2.3176(10)
Pt(1)-P(2)	2.3173(9)
Pt(1)-P(3)	2.3193(13)

P(1)-Pt(1)-P(2)	117.48(4)
P(1)-Pt(1)-P(3)	119.20(4)
P(2)-Pt(1)-P(3)	119.74(3)
Si(1)-Pt(1)-P(1)	83.46(4)
Si(1)-Pt(1)-P(2)	84.01(4)
Si(1)-Pt(1)-P(3)	83.58(5)

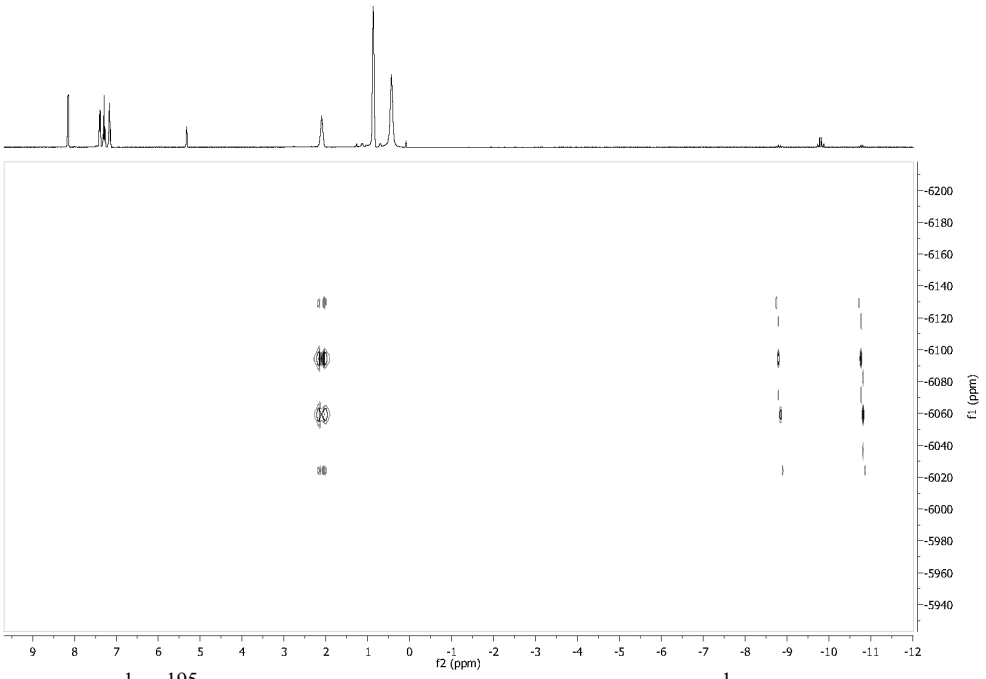

Figure S12. $^{1}H/^{195}Pt$ 2D HMBC NMR spectrum of **9**. ^{1}H NMR resonances along horizontal axis (f2) and ^{195}Pt NMR resonances along vertical axis (f1).

Table S8a. Crystal data and structure refinement for **10**.

Identification code	08289	
Empirical formula	C68 H66 B F24 P3 Pt Si	
Formula weight	1666.11	
Temperature	100(2) K	
Wavelength	0.71073 Å	
Crystal system	Monoclinic	
Space group	P2(1)/n	
Unit cell dimensions	a = 12.8824(10) Å	α = 90°.
	b = 38.101(3) Å	β = 92.5570(10)°.
	c = 14.3445(11) Å	γ = 90°.
Volume	7033.8(9) $Å^3$	
Z	4	
Density (calculated)	1.573 Mg/m^3	
Absorption coefficient	2.184 mm^{-1}	
F(000)	3328	
Crystal size	0.35 x 0.35 x 0.20 mm^3	
Theta range for data collection	1.07 to 30.60°.	
Index ranges	-18<=h<=18, -54<=k<=54, -20<=l<=20	
Reflections collected	194167	
Independent reflections	21476 [R(int) = 0.0614]	
Completeness to theta = 30.60°	99.1 %	
Absorption correction	Semi-empirical from equivalents	
Max. and min. transmission	0.6692 and 0.5153	
Refinement method	Full-matrix least-squares on F^2	
Data / restraints / parameters	21476 / 1940 / 915	
Goodness-of-fit on F^2	1.094	
Final R indices [I>2sigma(I)]	R1 = 0.0358, wR2 = 0.0720	
R indices (all data)	R1 = 0.0485, wR2 = 0.0767	
Largest diff. peak and hole	1.635 and -1.022 $e.Å^{-3}$	

Table S8b. Selected bond lengths [Å] and angles [°] for **10**.

Pt(1)-Si(1)	2.2594(7)	P(1)-Pt(1)-P(2)	119.61(3)
Pt(1)-P(1)	2.3618(7)	P(1)-Pt(1)-P(3)	119.84(2)
Pt(1)-P(2)	2.3743(7)	P(2)-Pt(1)-P(3)	118.59(2)
Pt(1)-P(3)	2.3830(7)	Si(1)-Pt(1)-P(1)	84.57(3)

Si(1)-Pt(1)-P(2)	85.97(3)	Si(1)-Pt(1)-P(3)	85.46(2)

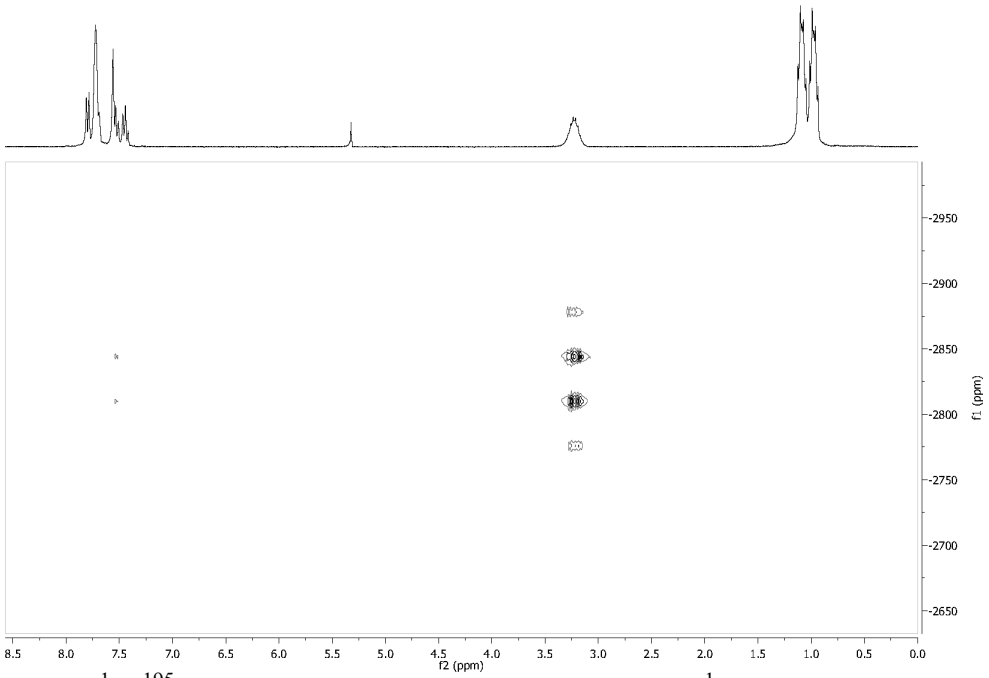

Figure S13. $^{1}H/^{195}Pt$ 2D HMBC NMR spectrum of **10**. ^{1}H NMR resonances along horizontal axis (f2) and ^{195}Pt NMR resonances along vertical axis (f1).

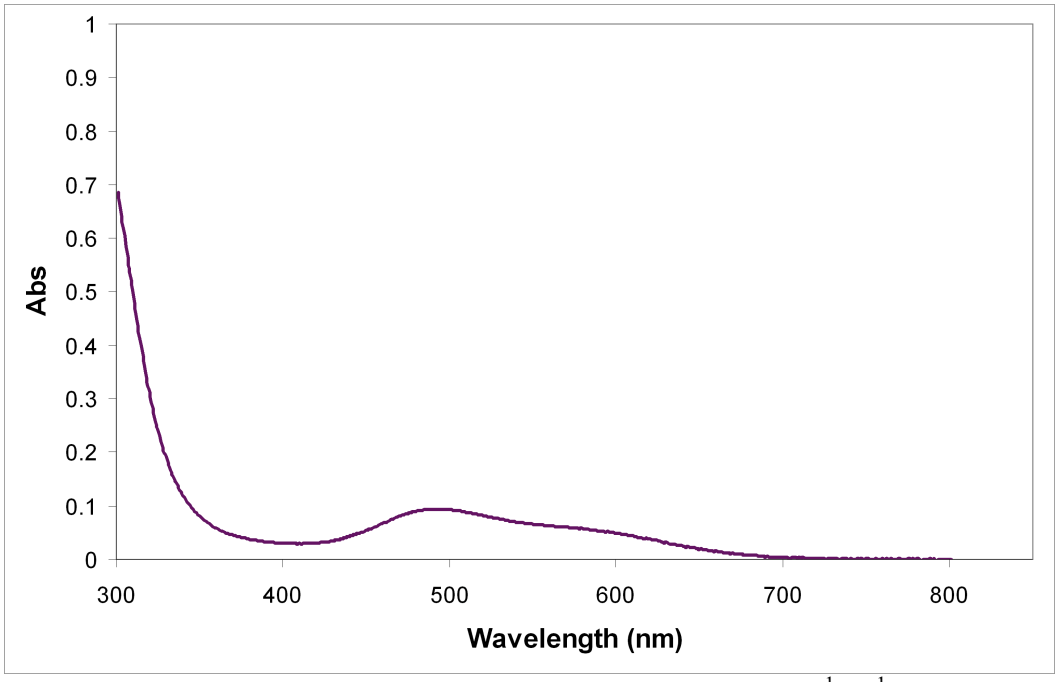

Figure S14. UV-visible spectrum of **10**. λ_{max} = 494 nm, ε = 964 cm^{-1} M^{-1}.

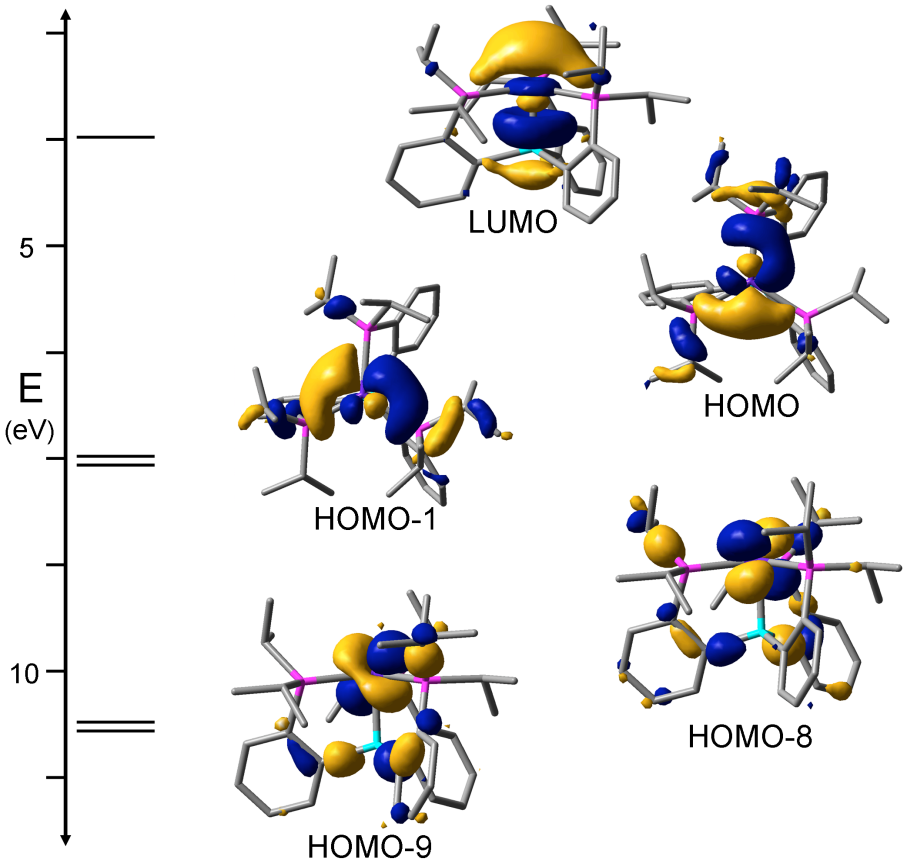

Figure S15. DFT-calculated frontier molecular orbitals of **10**. HOMO and HOMO-1 shown from top, looking down the Pt-Si axis; others shown from side-on view.

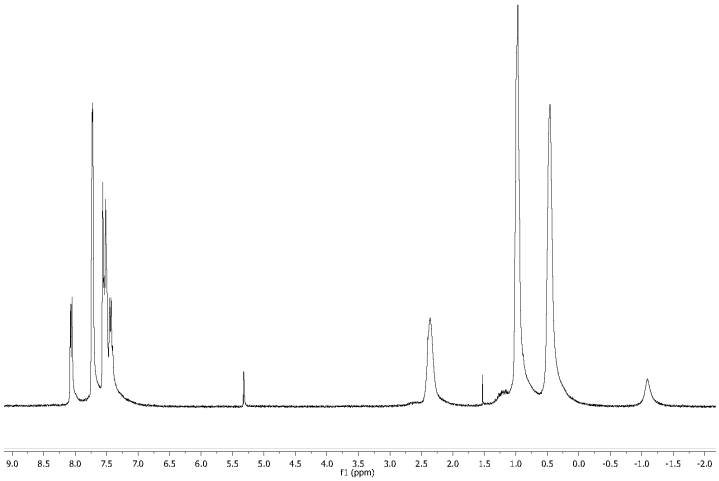

Figure S16a. ^{1}H NMR spectrum of **11** in CD_2Cl_2 at room temperature. The resonance for free H_2 is not observed due to its exchange with the bound H_2 (broad peak at -1.09 ppm).

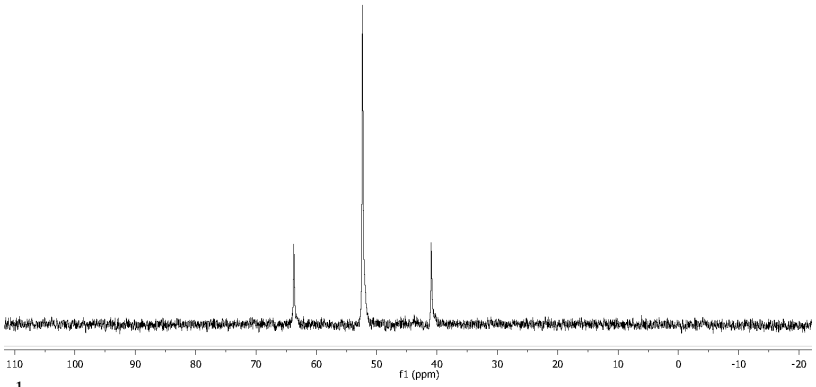

Figure S16b. ^{1}H NMR spectrum of **11** in CD_2Cl_2 at room temperature.

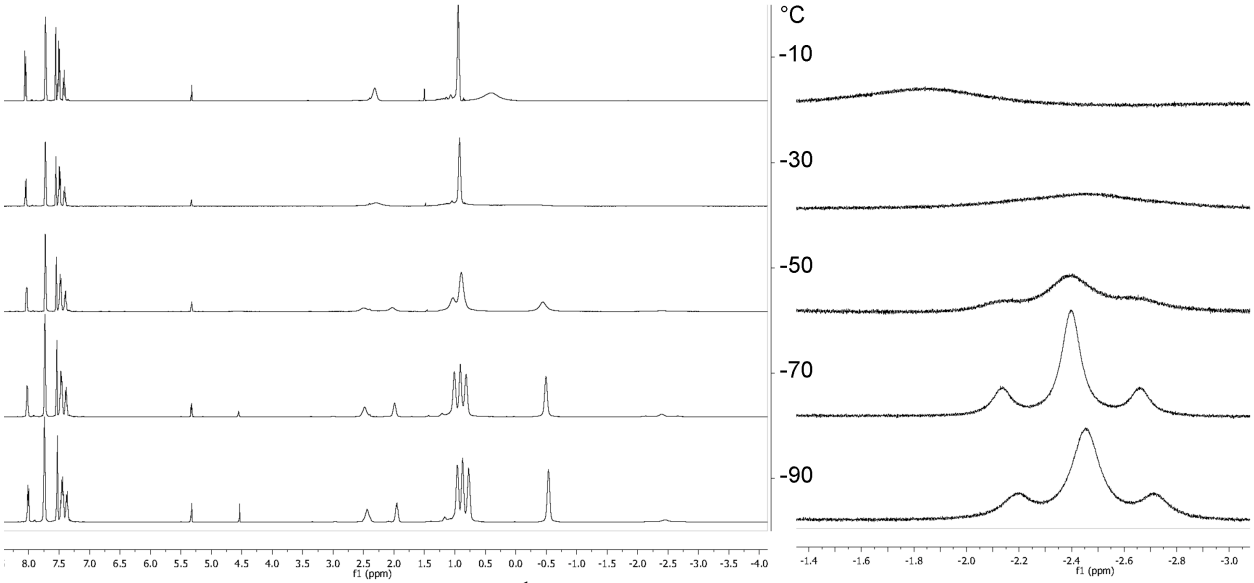

Figure S17. Variable-temperature ^{1}H NMR spectrum of **11a** in CD_2Cl_2 (500 MHz); blow-up of upfield region on right.

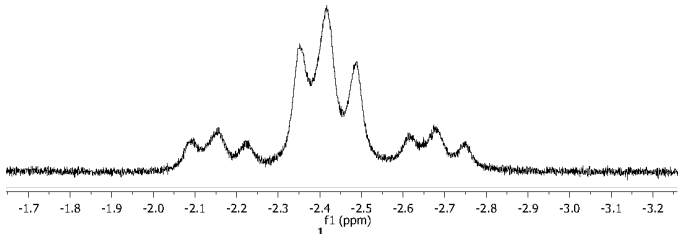

Figure S18. Blow-up of upfield region of ^{1}H NMR spectrum of **11b** at -70 °C in CD_2Cl_2 (500 MHz).

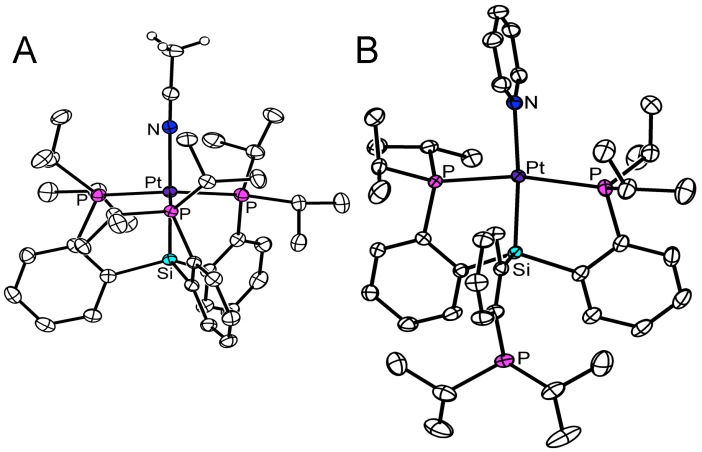

Figure S19. Solid-state structures of (A) **12** and (B) **13**. Thermal ellipsoids drawn at **50**% probability. Hydrogen atoms, solvent molecules, and BAr^F_4 anions omitted for clarity.

Table S9a. Crystal data and structure refinement for **12**.

Identification code	09111	
Empirical formula	C70 H69 B F24 N P3 Pt Si	
Formula weight	1707.16	
Temperature	100(2) K	
Wavelength	0.71073 Å	
Crystal system	Monoclinic	
Space group	P2(1)/c	
Unit cell dimensions	a = 12.8547(12) Å	α = 90°.
	b = 14.9356(13) Å	β = 96.574(2)°.
	c = 38.282(4) Å	γ = 90°.
Volume	7301.5(11) $Å^3$	
Z	4	
Density (calculated)	1.553 Mg/m^3	
Absorption coefficient	2.106 mm^{-1}	
F(000)	3416	
Crystal size	0.50 x 0.50 x 0.20 mm^3	
Theta range for data collection	1.07 to 29.57°.	
Index ranges	-17<=h<=17, -20<=k<=20, -52<=l<=53	
Reflections collected	161763	
Independent reflections	20461 [R(int) = 0.0612]	
Completeness to theta = 29.57°	99.9 %	
Absorption correction	Semi-empirical from equivalents	
Max. and min. transmission	0.6780 and 0.4190	

Refinement method	Full-matrix least-squares on F^2
Data / restraints / parameters	20461 / 759 / 963
Goodness-of-fit on F^2	1.060
Final R indices [I>2sigma(I)]	R1 = 0.0341, wR2 = 0.0706
R indices (all data)	R1 = 0.0474, wR2 = 0.0762
Largest diff. peak and hole	1.373 and -0.820 e.Å^{-3}

Table S9b. Selected bond lengths [Å] and angles [°] for **12**.

Pt(1)-N(1S)	2.175(2)
Pt(1)-Si(1)	2.2845(7)
Pt(1)-P(1)	2.3856(7)
Pt(1)-P(2)	2.3942(7)
Pt(1)-P(3)	2.3929(7)

N(1S)-Pt(1)-Si(1)	179.66(7)
P(1)-Pt(1)-P(2)	119.28(3)
P(3)-Pt(1)-P(2)	118.14(3)
P(1)-Pt(1)-P(3)	118.14(3)
N(1S)-Pt(1)-P(1)	96.92(6)
N(1S)-Pt(1)-P(2)	97.12(6)
N(1S)-Pt(1)-P(3)	97.09(6)
Si(1)-Pt(1)-P(1)	83.00(3)
Si(1)-Pt(1)-P(2)	82.63(3)
Si(1)-Pt(1)-P(3)	83.24(3)

Table S10a. Crystal data and structure refinement for **13**.

Identification code	09115	
Empirical formula	C73 H71 B F24 N P3 Pt Si	
Formula weight	1745.21	
Temperature	100(2) K	
Wavelength	0.71073 Å	
Crystal system	Triclinic	
Space group	P-1	
Unit cell dimensions	a = 12.9006(10) Å	α = 80.7460(10)°.
	b = 16.4405(13) Å	β = 88.5490(10)°.
	c = 17.9294(14) Å	γ = 81.5530(10)°.

Volume	3712.5(5) $Å^3$
Z	2
Density (calculated)	1.561 Mg/m^3
Absorption coefficient	2.073 mm^{-1}
F(000)	1748
Crystal size	0.50 x 0.40 x 0.20 mm^3
Theta range for data collection	1.27 to 29.57°.
Index ranges	-17<=h<=17, -22<=k<=22, -24<=l<=24
Reflections collected	83364
Independent reflections	20655 [R(int) = 0.0443]
Completeness to theta = 29.57°	99.2 %
Absorption correction	Semi-empirical from equivalents
Max. and min. transmission	0.6819 and 0.4237
Refinement method	Full-matrix least-squares on F^2
Data / restraints / parameters	20655 / 951 / 960
Goodness-of-fit on F^2	1.044
Final R indices [I>2sigma(I)]	R1 = 0.0314, wR2 = 0.0699
R indices (all data)	R1 = 0.0394, wR2 = 0.0740
Largest diff. peak and hole	1.316 and -0.719 $e.Å^{-3}$

Table S10b. Selected bond lengths [Å] and angles [°] for **13**.

Pt(1)-N(1)	2.222(2)
Pt(1)-Si(1)	2.3155(6)
Pt(1)-P(1)	2.3160(6)
Pt(1)-P(2)	2.3166(6)

N(1)-Pt(1)-Si(1)	173.23(6)
P(1)-Pt(1)-P(2)	162.46(2)
N(1)-Pt(1)-P(1)	92.49(5)
N(1)-Pt(1)-P(2)	101.10(5)
Si(1)-Pt(1)-P(1)	84.85(2)
Si(1)-Pt(1)-P(2)	82.78(2)

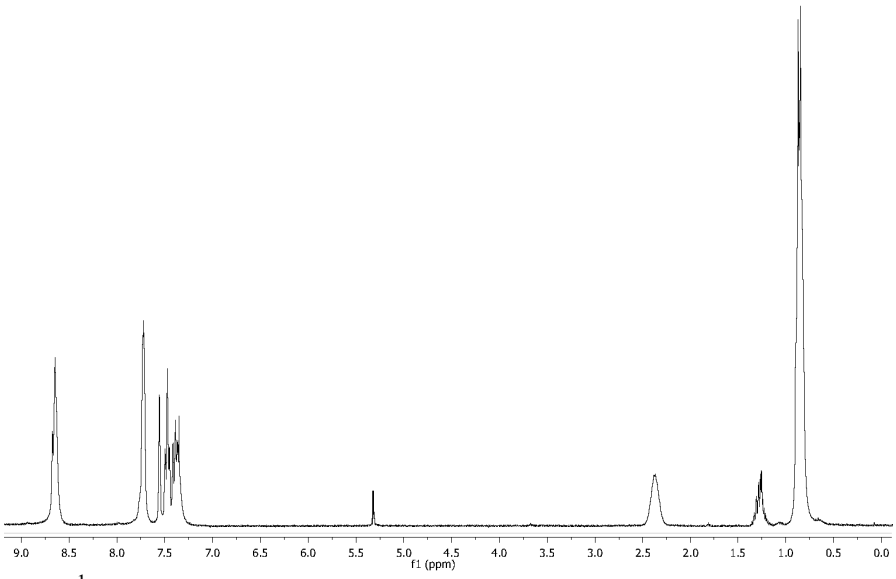

Figure S20a. ^{1}H NMR spectrum of **13** in CD_2Cl_2 at room temperature.

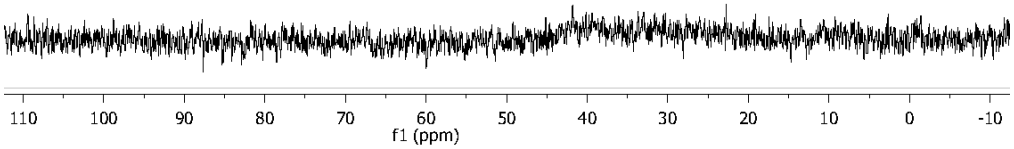

Figure S20b. $^{31}P\{^{1}H\}$ NMR spectrum of **13** in CD_2Cl_2; the fluxional nature of **13** at room-temperature results in a very broad resonance centered at approximately 40 ppm.

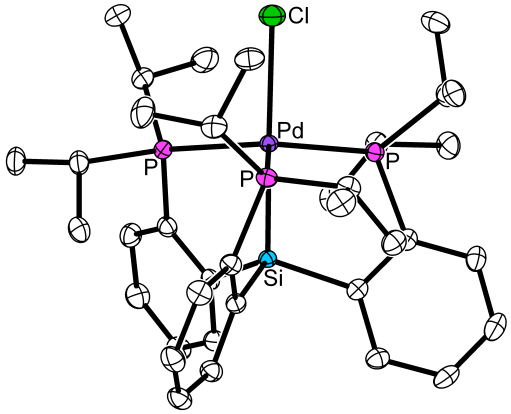

Figure S21. Solid-state structure of **15**. Thermal ellipsoids drawn at **50**% probability. Hydrogen atoms and solvent molecules omitted for clarity.

Table S11a. Crystal data and structure refinement for **15**.

Identification code	09202	
Empirical formula	C37 H56 Cl3 P3 Pd Si	
Formula weight	834.57	
Temperature	100(2) K	
Wavelength	0.71073 Å	
Crystal system	Monoclinic	
Space group	P2(1)/c	
Unit cell dimensions	a = 10.1305(7) Å	α = 90°.
	b = 24.594(2) Å	β = 91.071(2)°.
	c = 15.8544(13) Å	γ = 90°.
Volume	3949.4(5) $Å^3$	
Z	4	
Density (calculated)	1.404 Mg/m^3	
Absorption coefficient	0.850 mm^{-1}	
F(000)	1736	
Crystal size	0.48 x 0.25 x 0.18 mm^3	
Theta range for data collection	1.53 to 29.30°.	
Index ranges	-13<=h<=13, -33<=k<=33, -21<=l<=21	
Reflections collected	79812	
Independent reflections	10738 [R(int) = 0.0520]	
Completeness to theta = 29.30°	99.5 %	
Absorption correction	Semi-empirical from equivalents	
Max. and min. transmission	0.8620 and 0.6857	
Refinement method	Full-matrix least-squares on F^2	
Data / restraints / parameters	10738 / 312 / 418	
Goodness-of-fit on F^2	1.052	
Final R indices [I>2sigma(I)]	R1 = 0.0333, wR2 = 0.0751	
R indices (all data)	R1 = 0.0450, wR2 = 0.0820	
Largest diff. peak and hole	0.871 and -0.640 $e.Å^{-3}$	

Table S11b. Selected bond lengths [Å] and angles [°] for **15**.

Pd(1)-Cl(1)	2.5283(5)
Pd(1)-Si(1)	2.2763(5)
Pd(1)-P(1)	2.4088(6)
Pd(1)-P(2)	2.4207(5)

Pd(1)-P(3)	2.4160(6)
Si(1)-Pd(1)-Cl(1)	178.83(2)
P(3)-Pd(1)-P(2)	117.601(18)
P(1)-Pd(1)-P(2)	117.86(2)
P(1)-Pd(1)-P(3)	119.271(18)
P(1)-Pd(1)-Cl(1)	96.490(18)
P(2)-Pd(1)-Cl(1)	98.968(18)
P(3)-Pd(1)-Cl(1)	97.592(18)
Si(1)-Pd(1)-P(1)	82.682(18)
Si(1)-Pd(1)-P(2)	82.162(18)
Si(1)-Pd(1)-P(3)	82.122(18)

Table S12a. Crystal data and structure refinement for **16**.

Identification code	09089	
Empirical formula	C68 H66 B F24 P3 Pd Si	
Formula weight	1577.42	
Temperature	100(2) K	
Wavelength	0.71073 Å	
Crystal system	Monoclinic	
Space group	P2(1)/n	
Unit cell dimensions	a = 12.8728(10) Å	α = 90°.
	b = 38.131(3) Å	β = 92.3370(10)°.
	c = 14.4024(11) Å	γ = 90°.
Volume	7063.5(9) $Å^3$	
Z	4	
Density (calculated)	1.483 Mg/m^3	
Absorption coefficient	0.451 mm^{-1}	
F(000)	3200	
Crystal size	0.25 x 0.20 x 0.07 mm^3	
Theta range for data collection	1.07 to 30.03°.	
Index ranges	-18<=h<=18, -53<=k<=53, -20<=l<=20	
Reflections collected	157672	
Independent reflections	20623 [R(int) = 0.0703]	
Completeness to theta = 30.03°	99.7 %	
Absorption correction	Semi-empirical from equivalents	

Max. and min. transmission	0.9691 and 0.8956
Refinement method	Full-matrix least-squares on F^2
Data / restraints / parameters	20623 / 702 / 935
Goodness-of-fit on F^2	1.067
Final R indices [I>2sigma(I)]	R1 = 0.0483, wR2 = 0.1419
R indices (all data)	R1 = 0.0729, wR2 = 0.1603
Largest diff. peak and hole	0.917 and -0.757 e.Å^{-3}

Table S12b. Selected bond lengths [Å] and angles [°] for **16**.

Pd(1)-Si(1)	2.2506(7)
Pd(1)-P(1)	2.4338(7)
Pd(1)-P(2)	2.4383(7)
Pd(1)-P(3)	2.3988(7)

P(1)-Pd(1)-P(2)	117.61(2)
P(1)-Pd(1)-P(3)	119.04(3)
P(3)-Pd(1)-P(2)	120.38(2)
Si(1)-Pd(1)-P(1)	85.17(3)
Si(1)-Pd(1)-P(2)	84.29(2)
Si(1)-Pd(1)-P(3)	83.32(2)

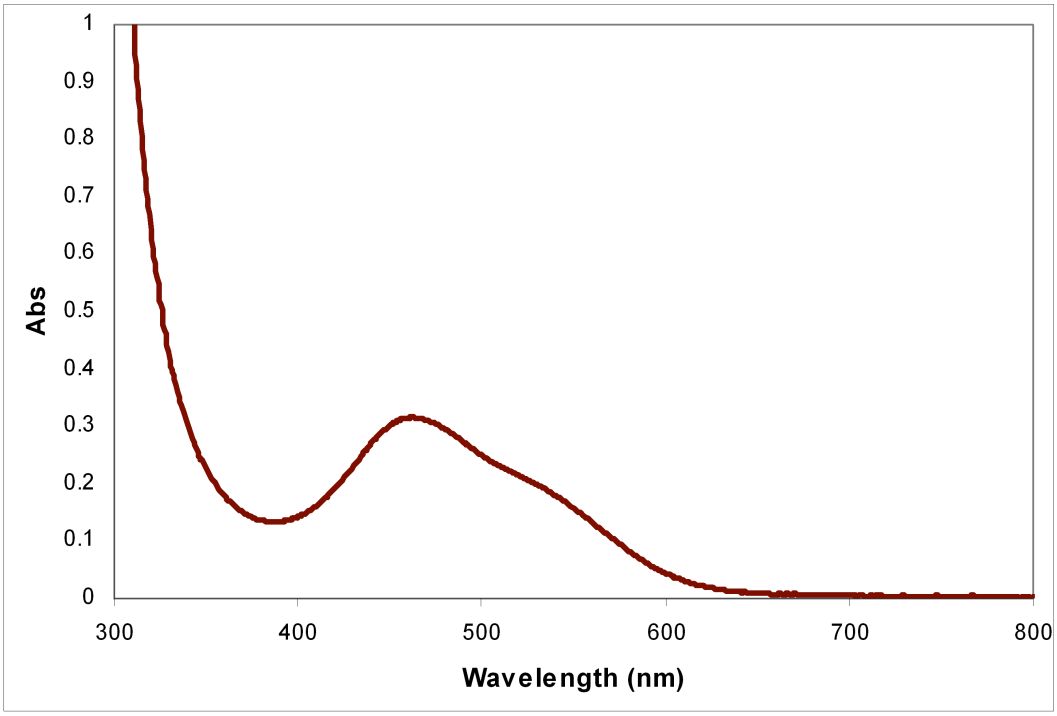

Figure S22. UV-visible spectrum of **16**. λ_{max} = 464 nm, ε = 931 cm^{-1} M^{-1}.

[1] Whited, M. T.; Mankad, N. P.; Lee, Y. H.; Oblad, P. F.; Peters, J. C. *Inorg. Chem.* **2009**, *48*, 2507-2517.
[2] Salo, E. V. and Guan, Z. *Organometallics* **2003**, *22*, 5033-5046.
[3] (a) Brookhart, M.; Grant, B.; Volpe, Jr., A. F. *Organometallics* **1992**, *11*, 3920-3922. (b) A solution of 1.2 M HCl in Et_2O was used instead of gaseous HCl.
[4] Implementation of "setref" is detailed in the Vnmr file found at /vnmr/nuctables/nuctabref.
[5] Harris, R. K.; Becker, E. D.; Cabral de Menezes, S. M.; Goodfellow, R.; Granger, P. *Pure Appl. Chem.* **2001**, *73*, 1795-1818.
[6] Sheldrick, G. M. *SHELXTL 2000*, Universität Göttingen: Göttingen, Germany, 2000.
[7] Frisch, M. J.; Trucks, G. W.; Schlegel, H. B.; Scuseria, G. E.; Robb, M. A.; Cheeseman, J. R.; Montgomery, J. A.; Vreven, T.; Kudin, K. N.; Burant, J. C.; Millam, J. M.; Iyengar, S. S.; Tomasi, J.; Barone, V.; Mennucci, B.; Cossi, M.; Scalmani, G.; Rega, N.; Petersson, G. A.; Nakatsuji, H.; Hada, M.; Ehara, M.; Toyota, K.; Fukuda, R.; Hasegawa, J.; Ishida, M.; Nakajima, T.; Honda, Y.; Kitao, O.; Nakai, H.; Klene, M.; Li, X.; Knox, J. E.; Hratchian, H. P.; Cross, J. B.; Adamo, C.; Jaramillo, J.; Gomperts, R.; Stratmann, R. E.; Yazyev, O.; Austin, A. J.; Cammi, R.; Pomelli, C.; Ochterski, J. W.; Ayala, P. Y.; Morokuma, K.; Voth, G. A.; Salvador, P.; Dannenberg, J. J.; Zakrzewski, V. G.; Dapprich, S.; Daniels, A. D.; Strain, M. C.; Farkas, O.; Malick, D. K.; Rabuck, A. D.; Raghavachari, K.; Foresman, J. B.; Ortiz, J. V.; Cui, Q.; Baboul, A. G.; Clifford, S.; Cioslowski, J.; Stefanov, B. B.; Liu, G.; Liashenko, A.; Piskorz, P.; Komaromi, I.; Martin, R. L.; Fox, D. J.; Keith, T.; Al-Laham, M. A.; Peng, C. Y.; Nanayakkara, A.; Challacombe, M.; Gill, P. M. W.; Johnson, B.; Chen, W.; Wong, M. W.; Gonzalez, C.; Pople, J. A. Gaussian 03; Revision B.05 ed.; Gaussian, Inc: Pittsburgh, PA, 2003.